JACS
JOURNAL OF THE AMERICAN CHEMICAL SOCIETY
Article
pubs.acs.org/JACS

ExCage

Edward J. Dale,[†] Nicolaas A. Vermeulen,[†] Andy A. Thomas,[§] Jonathan C. Barnes,[†,∥] Michal Juríček,[†,‡] Anthea K. Blackburn,[†] Nathan L. Strutt,[†] Amy A. Sarjeant,[†] Charlotte L. Stern,[†] Scott E. Denmark,[§] and J. Fraser Stoddart*[,†]

[†]Department of Chemistry, Northwestern University, 2145 Sheridan Road, Evanston, Illinois 60208, United States
[§]Department of Chemistry, University of Illinois, 505 South Mathews Avenue, Urbana, Illinois 61801, United States
[∥]Department of Chemistry, Massachusetts Institute of Technology, 77 Massachusetts Avenue, Cambridge, Massachusetts 02139, United States
[‡]Department of Chemistry, University of Basel, St. Johanns-Ring 19, 4056 Basel, Switzerland

Supporting Information

ABSTRACT: Cyclophanes, especially those where pyridinium units in conjugation with each other are linked up face-to-face within platforms that are held approximately 7 Å apart by rigid linkers, are capable of forming inclusion complexes with polycyclic aromatic hydrocarbons (PAHs) with high binding affinities as a result of a combination of noncovalent bonding interactions, including face-to-face [$\pi\cdots\pi$] stacking and orthogonal [C−H$\cdots\pi$] interactions. Here, we report the template-directed, catalyst-assisted synthesis of a three-fold symmetric, extended pyridinium-based, cage-like host (**ExCage**$^{6+}$) containing a total of six π-electron-deficient pyridinium units connected in a pairwise fashion by three bridging *p*-xylylene linkers, displayed in a trigonal (1,3,5) fashion around two opposing and parallel 1,3,5-tris(4-pyridinium)benzene platforms. The association constants (K_a) of eight complexes have been measured by isothermal titration calorimetry (ITC) in acetonitrile and were found to span the range from 2.82×10^3 for naphthalene up to 5.5×10^6 M^{-1} for perylene. The barriers to decomplexation, which were measured in DMF-d_7 for phenanthrene, pyrene, triphenylene, and coronene by dynamic ^{1}H NMR spectroscopy undergo significant stepwise increases from 11.8 → 13.6 → 15.5 → >18.7 kcal mol^{-1}, respectively, while complexation experiments using rapid injection ^{1}H NMR spectroscopy in DMF-d_7 at −55 °C revealed the barriers to complexation for pyrene and coronene to be 6.7 and >8 kcal mol^{-1}, respectively. The kinetic and thermodynamic data reveal that, in the case of **ExCage**$^{6+}$, while the smaller PAHs form complexes faster than the larger ones, the larger PAHs form stronger complexes than the smaller ones. It is also worthy of note that, as the complexes become stronger in the case of the larger and larger PAHs, the Rebek 55% solution formula for molecular recognition in the liquid state becomes less and less relevant.

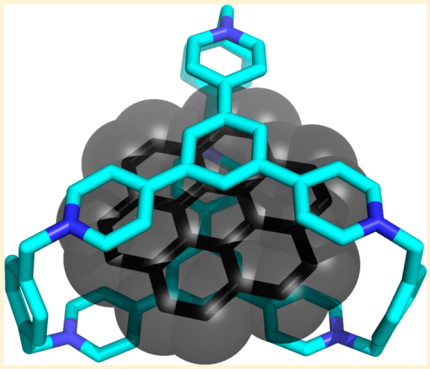

INTRODUCTION

No sooner had Pedersen[1] announced his landmark discovery[2] of the macrocyclic polyethers (crown ethers) in a seminal paper[3] in 1967, than did Lehn,[4] inspired by the synthesis and stereochemical properties of a family of macrobicylic diamines in 1968 by Simmons,[5] report[6] the preparation of the *N*,*N*′-diazamacrobicyclic polyethers (cryptands) in 1969. These three-dimensional analogues of the crown ethers bind Group IA and IIA metal cations so strongly that their 1:1 complexes became known as cryptates.[7] While the progression from crown ethers to cryptands occurred rapidly, it took quite a few years for the more highly designed spherands,[8] carcerands[9] and hemicarcerands,[10] introduced by Cram,[11] to make their entry on to the scene as hosts with concave inner surfaces that provide convergent recognition sites for the complexation of guests in the form of ions and neutral molecules with divergent binding sites. These early developments in host−guest chemistry[12] laid the foundations for the design and synthesis of cage-like host molecules[13] with constitutions ranging from being wholly organic[14] to being metal-coordinated.[15] These unnatural products, that fall under the umbrella of molecular cages, have been designed and synthesized for a vast range of different reasons including (i) exploring and exploiting their geometries,[16] (ii) studying their properties as molecular magnets,[17] (iii) employing them as molecular vehicles in the biomedical arena,[18] and (iv) using them to modulate and catalyze chemical reactions.[19]

Last year, we reported[20] on the efficient template-directed synthesis[21] of higher homologues of cyclobis(paraquat-*p*-phenylene)[22] (**CBPQT**$^{4+}$), resulting from extending both its bipyridinium units by inserting a *p*-phenylene ring between the two pyridinium rings in a stepwise fashion to produce extended tetracationic cyclophanes we have identified as **Ex^{n}Box**$^{4+}$, where

Received: April 28, 2014
Published: June 26, 2014

   dx.doi.org/10.1021/ja5041557 | J. Am. Chem. Soc. 2014, 136, 10669−10682

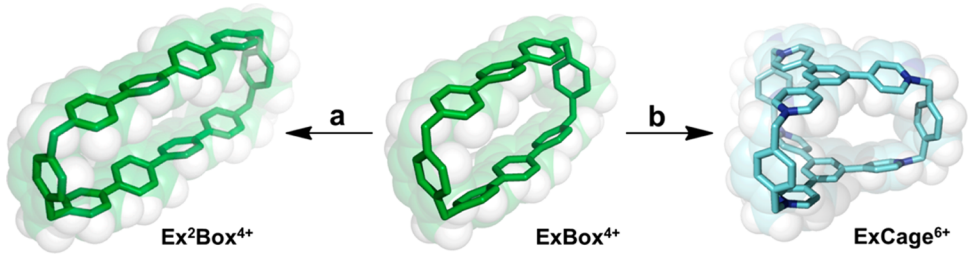

Figure 1. A perspective view of a stick diagram overlaid by a space-filling representation of the X-ray crystal structures of **ExBox**$^{4+}$, **Ex^{2}Box**$^{4+}$, and **ExCage**$^{6+}$. Synthetic analogues of cyclobis(paraquat-*p*-phenylene) can be achieved through the addition of central 1,4-disubstituted phenylene moieties. This extension, creating **ExBox**$^{4+}$ with a single addition, can be iterated (a) such that **Ex^{2}Box**$^{4+}$ or higher order **Ex^{n}Box**$^{4+}$ homologues are formed. Alternatively, (b) the substitution pattern of the central phenylene ring in **ExBox**$^{4+}$ can be altered to 1,3,5-trisubstituted, resulting in a bicyclic molecule with a cage-like constitution, **ExCage**$^{6+}$.

n = 0−3. If, instead of extending **ExBox**$^{4+}$ (where n = 1 and so the "1" is omitted from the acronym) in a linear fashion (Figure 1a) to produce **Ex^{2}Box**$^{4+}$, we change the constitution of the central 1,4-disubstituted benzenoid ring to one that is 1,3,5-trisubstituted, then we are clearly oriented (Figure 1b) in the direction of designing a bicyclic hexacationic cyclophane we have chosen to call **ExCage**$^{6+}$ for short. Herein, we report on (i) the template-directed synthesis of **ExCage**$^{6+}$ and (ii) its characterization by mass spectrometry in addition to NMR spectroscopy, single-crystal X-ray diffraction, and cyclic voltammetry, before describing (iii) its ability to form 1:1 complexes with no less than nine polycyclic aromatic hydrocarbons (PAHs), both in the solid state by X-ray crystallography and in solution by isothermal titration calorimetry (ITC). We also demonstrate (iv) that **ExCage**$^{6+}$ is able to extract naphthalene from an aqueous solution before describing (v) the kinetics of its complexation and decomplexation of selected PAH guests employing rapid injection and variable-temperature (VT) ^{1}H NMR spectroscopy, respectively.

In transporting the knowledge we have gained[20] during the past two years with "two-dimensional" **ExBox**$^{4+}$ hosts binding PAHs into the "three-dimensional" setting of **ExCage**$^{6+}$, we have come to realize that the kinetics and thermodynamics of the binding of PAHs, not only support, as expected, the operation of a macrobicyclic effect[6,7] but also raise fundamental questions relating to the subtle interplay between the enthalpies and entropies of binding and how they contribute to the free energies of binding. This interplay results in complexes that are, in general, entropically disfavored, as would be predicted by Rebek's 55% rule, given the large percentages of binding volumes that are occupied by the PAH guests. The larger PAH guests far surpass the entropic costs of binding with greater, favorable enthalpies of binding on account of the relatively high degree of molecular recognition built into **ExCage**$^{6+}$. Moreover, we have discovered that it becomes necessary to pay more attention to the kinetics of the binding process. In an attempt to bring all the thermodynamic and kinetic data together, we have found it useful, in interpreting the binding of PAHs by **ExCage**$^{6+}$ in both acetonitrile and *N*,*N*′-dimethylformamide solutions, to employ the concepts of *intrinsic* and *constrictive* binding introduced by Cram[11] in the context of binding very small organic molecules with hemicarerands. The fundamental point which emerges from our in-depth analysis of the data is that all-organic cages like **ExCage**$^{6+}$, which have portals with dimensions that restrict access into their cavities and a number of precisely located binding pockets that can act cooperatively, should allow smaller guests to form complexes faster than larger ones, while larger guests should form stronger complexes than smaller ones.

EXPERIMENTAL SECTION

The full experimental details are provided in the Supporting Information. The most important information is summarized below.

1,3,5-(1-(4-Bromomethylbenzyl)pyridinium-4-yl)benzene Tris(hexafluorophosphate) (TB·3PF$_6$). *α*,*α*′-Dibromo-*p*-xylene (8.96 g, 33.9 mmol) was added to MeCN/CH_2Cl_2 (2:1 v/v, 113 mL), and the suspension was heated at 60 °C until all of the compound had dissolved. The temperature of the solution was raised to 90 °C, and a suspension of 1,3,5-tris(4-pyridyl)benzene (**TP**) (700 mg, 2.26 mmol) in MeCN (37 mL) was added in aliquots during 2 h. After heating under reflux for 3 d, the reaction mixture was cooled to room temperature, and the precipitate was diluted in CH_2Cl_2 (500 mL) and collected by filtration. The precipitate was dissolved in MeOH (100 mL), followed by the addition of an excess of NH_4PF_6 in H_2O (400 mL), resulting in the precipitation of pure **TB**·3PF$_6$ (2.19 g, 75%) that was collected by filtration as a colorless solid. ^{1}H NMR (500 MHz, CD_3CN, ppm): δ_H 8.90 (AA′ of AA′XX′, J = 6.9 Hz, 6H), 8.53 (s, 3H), 8.49 (XX′ of AA′XX′, J = 6.9 Hz, 6H), 7.55 (AA′ of AA′BB′, J = 8.3 Hz, 6H), 7.49 (BB′ of AA′BB′, J = 8.2 Hz, 6H), 5.78 (s, 6H), 4.61 (s, 6H). ^{13}C NMR (125 MHz, CD_3CN, ppm): δ_C 155.9, 145.8, 141.3, 137.7, 134.1, 132.0, 131.1, 130.5, 127.4, 64.6, 33.5. HRMS-ESI for **TB**·3PF$_6$; Calcd for $C_{45}H_{39}Br_3F_{12}N_3P_2$: m/z = 1149.9952 $[M - PF_6]^+$; Found: 1149.9959 $[M - PF_6]^+$.

Cyclobis(1,3,5-tris(1,1′-(1,4-phenylenebis(methylene))-pyridinium-4-yl)benzene) Hexakis(hexafluorophosphate) (ExCage·6PF$_6$). Six reactions were carried out using different sets of conditions as follows: (i) catalyst with no template, (ii) no catalyst and no template, (iii) no catalyst and phenanthrene as template, (iv) no catalyst and pyrene as template, (v) catalyst and phenanthrene as template, and (vi) catalyst and pyrene as template.

(i) Catalyst with No Template. A solution of **TB**·3PF$_6$ (150 mg, 0.129 mmol), **TP** (39.7 mg, 0.129 mmol), and tetrabutylammonium iodide (TBAI, 14.2 mg, 0.0383 mmol) in dry MeCN (50 mL) was heated at 80 °C for 36 h. The reaction was quenched by addition of an excess of TBACl, whereupon the crude product precipitated from solution as the hexachloride salt, which was dissolved in the minimum amount of H_2O/EtOH (19:1, v/v) before being subjected to high-performance reverse-phase preparative C_{18} column chromatography, starting with H_2O containing 0.1% TFA as eluent, and adding up to 25% of MeCN/0.1% TFA. The chromatographically pure compound was precipitated by adding NH_4PF_6 to the eluent, affording pure **ExCage**·6PF$_6$ (15 mg, 7%). ^{1}H NMR (500 MHz, CD_3CN, ppm): δ_H 8.74 (AA′ of AA′XX′, J = 7.0 Hz, 12H), 8.40 (s, 6H), 8.28 (XX′ of AA′XX′, J = 6.6 Hz, 12H), 7.57 (s, 12H), 5.73 (s, 12H). ^{13}C NMR (125 MHz, CD_3CN, ppm): δ_C 154.2, 145.3, 136.9, 136.7, 131.6, 131.4, 126.5, 64.7. HRMS-ESI for **ExCage**·6PF$_6$; Calcd for $C_{66}H_{54}F_{24}N_6P_4$: m/z = 755.1483 $[M - 2PF_6]^{2+}$; Found: 755.1505 $[M - 2PF_6]^{2+}$.

(ii) No Catalyst and No Template. A solution of **TB**·3PF$_6$ (1 equiv) and **TP** (1 equiv) in dry MeCN was stirred at room temperature for 21 days. The reaction was worked up as described in (i) above to give trace amounts of **ExCage**·6PF$_6$.

(iii) No Catalyst and Phenanthrene as Template. A solution of **TB**·3PF$_6$ (1 equiv), **TP** (1 equiv), and phenanthrene (6 equiv) in dry MeCN

dx.doi.org/10.1021/ja5041557 | J. Am. Chem. Soc. 2014, 136, 10669−10682

was stirred at room temperature for 21 days. The reaction was quenched by adding an excess of TBACl, whereupon the crude product precipitated from solution as the hexachloride salt. The template was removed by continuous liquid–liquid extraction with $CHCl_3$ over the course of 3 days. The resultant aqueous phase was concentrated to give a crude residue containing **ExCage**·6Cl, which was subjected to chromatography and counterion exchange as described above in (i) to afford pure **ExCage**·6PF_6 in 9% yield.

(iv) No Catalyst and Pyrene as Catalyst. The same protocol was followed as described in (iii), with phenanthrene being replaced by pyrene and continuous liquid–liquid extraction with $CHCl_3$ requiring 30 days, to afford pure **ExCage**·6PF_6 in 11% yield.

(v) Catalyst and Phenanthrene as Template. By combining the protocols described in (i) and (iii) above, **ExCage**·6PF_6 was isolated in 35% yield.

(vi) Catalyst and Pyrene as Template. By combining the protocols described in (i) and (iv) above, **ExCage**·6PF_6 was isolated in 45% yield.

Single-Crystal X-ray Diffraction (XRD). Single crystals of **ExCage**·6PF_6 and its 1:1 complexes with PAHs were grown by slow vapor diffusion of iPr$_2$O into solutions of **ExCage**·6PF_6, or the host, with the PAH guests in considerable excess in MeCN over the course of hours to days. Data were collected at 100 K on a Bruker Kappa APEX2 CCD Diffractometer equipped with a CuKα microsource with Quazar or MX optics. Crystallographic data are available free of charge from the Cambridge Crystallographic Data Centre (CCDC) using www.ccdc.cam.ac.uk/data_request/cif. The experimental methods employed to obtain the single crystals, along with the crystal data and its refinement in each case will now be presented.

ExCage·6PF_6. The cage (0.9 mg, 0.5 μmol) was dissolved in MeCN (0.2 mL), and the solution was passed through a 0.45 μm filter into a 1 mL tube, which was placed inside a 7.5 mL vial containing iPr$_2$O (1 mL). The vial was capped, and after slow vapor diffusion of iPr$_2$O at room temperature into the MeCN solution for a day, yellow single crystals of **ExCage**·6PF_6, suitable for X-ray crystallography, were obtained. Crystal parameters: $[C_{70}H_{60}N_6\cdot(PF_6)_6]\cdot(MeCN)_2$. Yellow block (0.43 × 0.34 × 0.31 mm). Orthorhombic, *Cmcm*, a = 18.042(7), b = 28.495(14), c = 21.530(7) Å, α = 90.000, β = 108.579(3), γ = 90.000°, V = 11068.8(8) Å^3, Z = 4, T = 100.15 K, ρ_{calc} = 1.130 g cm^{-3}, μ = 0.192 mm^{-1}. Of a total of 6811 reflections that were collected, 4642 were unique. Final R_1 = 0.1150 and wR_2 = 0.3324. The solvent-masking procedure in Olex2 was used[23] to remove the electronic contributions from the disordered solvent molecules. The total solvent accessible volume per cell is 4135.0 Å^3 (37.4%) with a total electron count per cell of 608.9. CCDC number: 988434.

Naphthalene⊂ExCage·6PF_6. Naphthalene (0.25 mg, 2.2 μmol) was added in a 4:1 ratio to a solution of **ExCage**·6PF_6 (1.0 mg, 0.55 μmol) in MeCN (1.0 mL). After the PAH had dissolved, the solution was passed through a 0.45 μm filter into a 2 dram vial which was placed in a 20 mL vial containing iPr$_2$O (3 mL). The vial was capped, and after slow vapor diffusion of iPr$_2$O at room temp into the MeCN solution for 2 d, colorless single crystals of naphthalene⊂**ExCage**·6PF_6, suitable for X-ray crystallography, were obtained. Crystal parameters: $C_{10}H_8\subset C_{66}H_{54}N_6\cdot(PF_6)_6]\cdot(MeCN)_3$. Colorless block (0.42 × 0.20 × 0.18 mm). Orthorhombic, *Cmcm*, a = 18.085(5), b = 28.501(8), c = 21.571(6) Å, α = 90.000, β = 90.000, γ = 90.000°, V = 11118.3(5) Å^3, Z = 4, T = 99.99 K, ρ_{calc} = 1.188 g cm^{-3}, μ = 1.789 mm^{-1}. Of a total of 95509 reflections that were collected, 5324 were unique. Final R_1 = 0.0696 and wR_2 = 0.2293. Rigid-bond restraints were imposed on the displacement parameters in addition to restraints on similar amplitudes separated by <1.7 Å on the disordered PF_6^- anions and the naphthalene. Distance restraints were also imposed[24] on the naphthalene. The solvent-masking procedure as implemented[23] in Olex2 was used to remove the electronic contribution of the solvent molecules from the refinement. Since the exact solvent content was unknown, only the atoms used in the refinement model are reported in the formula. The total solvent accessible volume per cell is 2713.0 Å^3 (24.4%) with a total electron count per cell of 673.8. CCDC number: 988435.

Phenanthrene⊂ExCage·6PF_6. Phenanthrene (0.25 mg, 1.4 μmol) was added in a ratio of 20:1 to a solution of **ExCage**·6PF_6 (0.13 mg, 0.073 μmol) in MeCN (0.05 mL), and after the PAH had dissolved, the solution was passed through a 0.45 μm filter into a 1 mL tube which was placed in a 7.5 mL vial containing iPr$_2$O (1 mL). The vial was capped, and after slow vapor diffusion of iPr$_2$O at room temperature into the MeCN solution for 2 d, yellow single crystals of phenanthrene⊂**ExCage**·6PF_6, suitable for X-ray crystallography, were obtained. Crystal parameters: $[C_{14}H_{10}\subset C_{66}H_{54}N_6\cdot(PF_6)_6]\cdot(MeCN)_3$. Yellow block (0.29 × 0.24 × 0.03 mm). Orthorhombic, *Pbcm*, a = 18.103(12), b = 28.586(2), c = 21.373(13) Å, α = 90.000, β = 90.000, γ = 90.000°, V = 11060.4(13) Å^3, Z = 4, T = 100.0 K, ρ_{calc} = 1.263 g cm^{-3}, μ = 1.828 mm^{-1}. Of a total of 64749 reflections that were collected, 9709 were unique. Final R_1 = 0.1084 and wR_2 = 0.3388. The enhanced rigid-bond restraint was applied[2S] globally. Chemically equivalent, but not symmetry-equivalent, phenanthrene atoms were restrained so that bond distances and angles were similar to one another. Rigid-bond restraints were imposed on the displacement parameters in addition to restraints on similar amplitudes separated by <1.7 Å on disordered phenanthrene molecules. The solvent-masking procedure as implemented[23] in Olex2 was used to remove the electronic contribution of the solvent molecules from the refinement. The total solvent accessible volume per cell is 2169.3 Å^3 (19.8%) with a total electron count per cell of 263.5. Since the exact solvent content was unknown, only the atoms used in the refinement model are reported in the formula. CCDC number: 988436.

Chrysene⊂ExCage·6PF_6. Chrysene (1.2 mg, 5.3 μmol) was added in a ratio of 15:1 to a solution of **ExCage**·6PF_6 (0.60 mg, 0.33 μmol) in MeCN (0.2 mL), and after the PAH had dissolved, the solution was passed through a 0.45 μm filter into a 1 mL tube which was placed in a 7.5 mL vial containing iPr$_2$O (1 mL). The vial was capped, and after slow vapor diffusion of iPr$_2$O at room temperature into the MeCN solution for 3 d, yellow single crystals of chrysene⊂**ExCage**·6PF_6, suitable for X-ray crystallography, were obtained. Crystal parameters: $[C_{18}H_{12}\subset C_{66}H_{54}N_6\cdot(PF_6)_6]\cdot(MeCN)_{10}$. Yellow block (0.28 × 0.24 × 0.10 mm). Orthorhombic, *Cmc*2$_1$, a = 18.142(6), b = 28.462(9), c = 21.328(6) Å, α = 90.000, β = 90.000, γ = 90.000°, V = 11013.3(6) Å^3, Z = 4, T = 99.99 K, ρ_{calc} = 1.471 g cm^{-3}, μ = 1.939 mm^{-1}. Of a total of 45546 reflections that were collected, 9812 were unique. Final R_1 = 0.0456 and wR_2 = 0.1232. Similar distance restraints were applied to chemically equivalent 1,2-, 1,3-, and 1,4-C–C distances in the case of the disordered chrysene molecule. Displacement parameters for the chrysene carbon atoms were subjected[24] to rigid-bond restraint. CCDC number: 988437.

Tetraphene⊂ExCage·6PF_6. Tetraphene (0.66 mg, 2.9 μmol) was added in a ratio of 9:1 to a solution of **ExCage**·6PF_6 (0.60 mg, 0.33 μmol) in MeCN (0.2 mL), and after the PAH had dissolved, the solution was passed through a 0.45 μm filter into a 1 mL tube which was placed in a 7.5 mL vial containing iPr$_2$O (1 mL). The vial was capped, and after slow vapor diffusion of iPr$_2$O at room temperatre into the MeCN solution for 3 d, yellow single crystals of tetraphene⊂**ExCage**·6PF_6, suitable for X-ray crystallography, were obtained. Crystal parameters: $[C_{18}H_{12}\subset C_{66}H_{54}N_6\cdot(PF_6)_6]\cdot(MeCN)_2$. Yellow block (0.25 × 0.16 × 0.12 mm). Orthorhombic, *Cmcm*, a = 18.157(8), b = 28.663(13), c = 21.162(10) Å, α = 90.000, β = 90.000, γ = 90.000°, V = 11012.9(9) Å^3, Z = 4, T = 100.01 K, ρ_{calc} = 1.205 g cm^{-3}, μ = 1.807 mm^{-1}. Of a total of 26346 reflections that were collected, 4909 were unique. Final R_1 = 0.0958 and wR_2 = 0.3104. The solvent-masking procedure as implemented[23] in Olex2 was used to remove the electronic contribution of solvent molecules from the refinement. Since the exact solvent content was unknown, only the atoms used in the refinement model are reported in the formula. The total solvent accessible volume is 2456.7 Å^3 (22.3%) with a total electron count of 475.8 per cell. CCDC number: 988438.

Helicene⊂ExCage·6PF_6. Helicene (1.2 mg, 5.3 μmol) was added in a ratio of 10:1 to a solution of **ExCage**·6PF_6 (1.0 mg, 0.56 μmol) in MeCN (0.2 mL), and after the PAH had dissolved, the solution was passed through a 0.45 μm filter into a 1 mL tube which was placed in a 7.5 mL vial containing iPr$_2$O (1 mL). The vial was capped, and after slow vapor diffusion of iPr$_2$O at room temperature into the MeCN solution for 3 d, yellow single crystals of helicene⊂**ExCage**·6PF_6, suitable for X-ray crystallography, were obtained. $[C_{18}H_{12}\subset C_{66}H_{54}N_6\cdot(PF_6)_6]\cdot(MeCN)_7$. Yellow block (0.30 × 0.23 × 0.14 mm). Monoclinic, $P2_1/n$, a = 18.268(8), b = 30.738(12), c = 21.501(9) Å, α = 90.000, β =

dx.doi.org/10.1021/ja5041557 | J. Am. Chem. Soc. 2014, 136, 10669–10682

111.192(2), γ = 90.000°, V = 11256.8(8) Å^3, Z = 4, T = 100.01 K, ρ_{calc} = 1.384 g cm^{-3}, μ = 1.860 mm^{-1}. Of a total of 77915 reflections that were collected, 19974 were unique. Final R_1 = 0.0933 and wR_2 = 0.2456. Similar distance restraints were applied to all disordered atoms. A group displacement parameter was used to refine the atoms of the minor component of the disordered helicene molecules. Rigid-bond and similarity restraints were used[25] to refine the displacement parameters of the major helicene component. The solvent-masking procedure as implemented in Olex2 was used to remove the electronic contribution of the solvent molecules from the refinement. The formula reported reflects the 28 MeCN molecules removed by this treatment. The total solvent accessible volume is 3605.0 Å^3 (32.0%) with a total electron count of 642.8 per cell. CCDC number: 988439.

Pyrene⊂ExCage·6PF$_6$. Pyrene (2.2 mg, 11 μmol) was added in a ratio of 40:1 to a solution of **ExCage**·6PF$_6$ (0.46 mg, 0.26 μmol) in MeCN (0.2 mL), and after the PAH had dissolved, the solution was passed through a 0.45 μm filter into a 1 mL tube which was placed in a 7.5 mL vial containing iPr$_2$O (1 mL). The vial was capped, and after slow vapor diffusion of iPr$_2$O at room temperature into the MeCN solution for 2 d, orange single crystals of the pyrene⊂**ExCage**·6PF$_6$, suitable for X-ray crystallography, were obtained. Crystal parameters: [C$_{16}$H$_{10}$⊂C$_{66}$H$_{54}$N$_6$·(PF$_6$)$_6$]·(MeCN)$_2$. Orange block (0.25 × 0.16 × 0.12 mm). Orthorhombic, *Cmcm*, a = 18.035(6), b = 28.636(10), c = 21.362(7) Å, α = 90.000, β = 90.000, γ = 90.000°, V = 11032.8(6) Å^3, Z = 4, T = 100.01 K, ρ_{calc} = 1.255 g cm^{-3}, μ = 1.826 mm^{-1}. Of a total of 22229 reflections that were collected, 4243 were unique. Final R_1 = 0.1076 and wR_2 = 0.3413. Distance restraints were imposed on similar distances of the disordered atoms. Rigid-bond restraints were imposed[25] on the displacement parameters in addition to restraints on similar amplitudes separated by <1.7 Å on the disordered atoms. The solvent-masking procedure as implemented in Olex2 was used[23] to remove the electronic contribution of solvent molecules from the refinement. Since the exact solvent content was unknown, only the atoms used in the refinement model are reported with the formula. The total solvent accessible volume is 2763.3 Å^3 (25.0%) with a total electron count of 675.9 per cell. CCDC number: 988440.

Triphenylene⊂ExCage·6PF$_6$. Triphenylene (0.42 mg, 1.9 μmol) was added in a ratio of 2:1 to a solution of **ExCage**·6PF$_6$ (1.7 mg, 0.95 μmol) in MeCN (0.2 mL), and after the PAH had dissolved, the solution was passed through a 0.45 μm filter into a 1 mL tube which was placed in a 7.5 mL vial containing iPr$_2$O (1 mL). The vial was capped, and after slow vapor diffusion of iPr$_2$O at room temperature into the MeCN solution for 1 d, yellow single crystals of triphenylene⊂**ExCage**·6PF$_6$, suitable for X-ray crystallography were obtained. Crystal parameters: [C$_{18}$H$_{12}$⊂C$_{66}$H$_{54}$N$_6$·(PF$_6$)$_6$]·(MeCN)$_{12}$. Yellow block (0.45 × 0.21 × 0.09 mm). Trigonal, $R\bar{3}$, a = 30.624(5), b = 30.6242(5), c = 20.967(5) Å, α = 90.000, β = 90.000, γ = 120.000°, V = 17029.4(7) Å^3, Z = 6, T = 99.99 K, ρ_{calc} = 1.475 g cm^{-3}, μ = 1.906 mm^{-1}. Of a total of 27599 reflections that were collected, 6333 were unique. Final R_1 = 0.0435 and wR_2 = 0.1253. No special refinement of the data was necessary. CCDC number: 988441.

Perylene⊂ExCage·6PF$_6$. Perylene (0.042 mg, 0.16 μmol) was added in a ratio of 1.9:1 to a solution of **ExCage**·6PF$_6$ (0.15 mg, 0.083 μmol) in MeCN (0.2 mL), and after some of the PAH had dissolved, the solution was passed through a 0.45 μm filter into a 1 mL tube which was placed in a 7.5 mL vial containing iPr$_2$O (1 mL). The vial was capped, and after slow vapor diffusion of iPr$_2$O at room temperature into the MeCN solution for 12 h, red single crystals of perylene⊂**ExCage**·6PF, suitable for X-ray crystallography, were obtained. Crystal parameters: [C$_{20}$H$_{12}$⊂C$_{66}$H$_{54}$N$_6$·(PF$_6$)$_6$]·(MeCN)$_2$. Red block (0.07 × 0.06 × 0.01 mm). Orthorhombic, *Cmcm*, a = 18.078(18), b = 28.704(2), c = 21.242(2) Å, α = 90.000, β = 95.911(2), γ = 90.000°, V = 11022.7(17) Å^3, Z = 4, T = 100.01 K, ρ_{calc} = 1.287 g cm^{-3}, μ = 1.841 mm^{-1}. Of a total of 23404 reflections that were collected, 4740 were unique. Final R_1 = 0.0819 and wR_2 = 0.2204. Rigid-bond restraints were imposed[25] on the displacement parameters in addition to restraints on similar amplitudes separated by <1.7 Å on the disordered perylene. Also, distances between carbon bonds in the perylene molecule were restrained to be similar. The solvent-masking procedure as implemented in Olex2 was used[23] to remove the electronic contribution of solvent molecules from the refinement. Since the exact solvent content was unknown, only the atoms used in the refinement model are reported in the formula. The total solvent accessible volume is 2542.6 Å^3 (23.1%) with a total electron count of 116.4 per cell. CCDC number: 988442.

Coronene⊂ExCage·6PF$_6$. Coronene (1.4 mg, 4.7 μmol) was added in a ratio of 10:1 to a solution of **ExCage**·6PF$_6$ (0.85 mg, 0.047 μmol) in MeCN (0.2 mL) and was heated at 80 °C for 1 min. After some of the PAH had dissolved following the heat treatment, the solution was passed through a 0.45 μm filter into a 1 mL tube which was placed in a 7.5 mL vial containing iPr$_2$O (1 mL). The vial was capped, and after slow vapor diffusion of iPr$_2$O at room temperature into the MeCN solution for 5 d, yellow single crystals of coronene⊂**ExCage**·6PF$_6$, suitable for X-ray crystallography, were obtained. Crystal parameters: [C$_{24}$H$_{12}$⊂C$_{66}$H$_{54}$N$_6$·(PF$_6$)$_6$]. Yellow block (0.27 × 0.15 × 0.08 mm). Monoclinic, *C*2/*m*, a = 23.134(18), b = 30.560(2), c = 18.206(11) Å, α = 90.000, β = 120.575(5), γ = 90.000°, V = 11061.0(15) Å^3, Z = 4, T = 100.00 K, ρ_{calc} = 1.262 g cm^{-3}, μ = 1.822 mm^{-1}. Of a total of 8262 reflections that were collected, 8262 were unique. Final R_1 = 0.1119 and wR_2 = 0.2992. The enhanced rigid-bond restraint was applied[25] globally. Additional rigid-bond and similarity restraints were[24] applied to disordered atoms. Disordered PF$_6^-$ anions were refined with similar distance restraints to regularize their octahedral geometry. The crystal used for experimentation was found to be nonmerohedrally twinned in three components. The final twin laws were determined through the integration program (SAINT) as −0.59606 −0.49399 −1.09681/−0.40527 −0.49928 1.12205/−0.40339 0.49062 0.09535 and −0.59911 0.49113 −1.10133/0.40607 −0.50179 −1.11870/−0.40073 −0.49055 0.10091 for the first-to-second and first-to-third component transformations. The twin fractions for the second and third components refined to 0.342(4) and 3.12(3), respectively. The program SQUEEZE (PLATON) was used[26] to remove electronic contributions from disordered solvent molecules. A total of 897 electrons per cell were removed from a void volume of 3314.9 Å^3. CCDC number: 988443.

Cyclic Voltammetry (CV). CV was carried out at room temperature in Ar-purged solutions of DMF with a Gamry multipurpose instrument (reference 600) interfaced to a PC. All CV experiments were performed using a glassy carbon working electrode (0.071 cm^2). The electrode surface was polished routinely with 0.05 μm alumina−H$_2$O slurry on a felt surface immediately before use. The counter electrode was a Pt coil, and the reference electrode was a Ag/AgCl one. The concentration of the sample and supporting electrolyte, tetrabutylammonium hexafluorophosphate (TBAPF$_6$), was 1.0 mM and 0.10 M, respectively. The CV cell was dried in an oven immediately before use, and Ar was flushed continuously through the cell as it was cooled down to room temperature to avoid condensation of water.

Isothermal Titration Calorimetry (ITC). ITC experiments were performed on a MicroCal system, VP-ITC model. A solution of **ExCage**·6PF$_6$ in MeCN (or DMF) was employed as the host solution in a 1.8 mL cell. Solutions of PAHs in MeCN (or DMF) were added by injecting successively 10 μL of titrant over 20 s (25×) with a 300 s interval between each injection. Thermodynamic information was calculated employing a one-site binding model utilizing data from which the heat of dilution of the guest was subtracted, with the average of triplet runs being reported.

Rapid Injection Nuclear Magnetic Resonance Spectroscopy (RI-NMR). In order to investigate the real-time formation of inclusion complexes between **ExCage**$^{6+}$ and selected PAH guests, an RI-NMR apparatus developed[27] in the Denmark laboratories at the University of Illinois at Urbana−Champaign (UIUC) was called into action. The apparatus uses a ceramic pump (IVEK Dispense 2000) to inject reagent solutions accurately into a spinning (20 Hz) 5 mm NMR tube containing the substrate inside the probe of a 600 MHz Varian NMR spectrometer. Two pneumatic pumps are used to control the injector tip into the solution and back to the resting position independently. The injector tip and tube, manufactured from titanium, are housed in a high-density polycarbonate sheathe, which guides the injector into the NMR tube inside the NMR spectrometer. An S-shaped paddle on the tip of the injector with three delivery ports 120° apart injects radially to aid in mixing. These parts are coordinated in a central control module such that a predetermined volume can be dispensed, while the injector tip is

Scheme 1. The Templated-Directed Synthesis of ExCage·6PF$_6$[a]

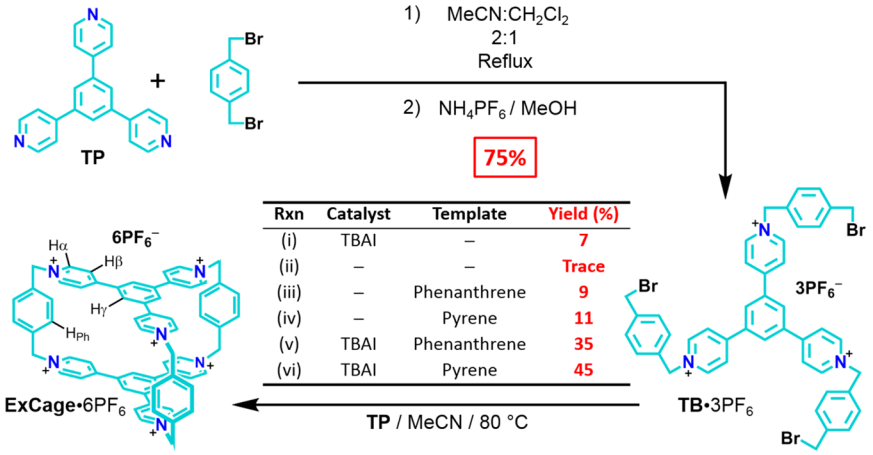

[a]Reagents and conditions: (i) (a) **TP** (1 equiv), **TB**·3PF$_6$ (1 equiv), TBAI (0.3 equiv), MeCN, 80 °C, 36 h; (b) Excess TBACl, H$_2$O/EtOH (19:1, v/v); (c) HPLC; (d) NH$_4$PF$_6$/Eluent. (ii) (a) **TP** (1 equiv), **TB**·3PF$_6$ (1 equiv), MeCN, rt, 21 days; (b) Excess TBACl, H$_2$O/EtOH (19:1, v/v); (c) HPLC; (d) NH$_4$PF$_6$/Eluent. (iii) (a) **TP** (1 equiv), **TB**·3PF$_6$ (1 equiv), phenanthrene (6 equiv), MeCN, rt, 21 days; (b) Excess TBACl, H$_2$O; (c) Liquid/liquid extraction/CHCl$_3$; (d) HPLC; (e) NH$_4$PF$_6$/Eluent. (iv) (a) **TP** (1 equiv), **TB**·3PF$_6$ (1 equiv), pyrene (6 equiv), MeCN, rt, 21 days; (b) Excess TBACl, H$_2$O; (c) Liquid/liquid extraction/CHCl$_3$; (d) HPLC; (e) NH$_4$PF$_6$/Eluent. (v) (a) **TP** (1 equiv), **TB**·3PF$_6$ (1 equiv), TBAI (0.3 equiv), phenanthrene (6 equiv), MeCN, 80 °C, 36 h; (b) Excess TBACl, H$_2$O; (c) Liquid/liquid extraction/CHCl$_3$; (d) HPLC; (e) NH$_4$PF$_6$/Eluent. (vi) (a) **TP** (1 equiv), **TB**·3PF$_6$ (1 equiv), TBAI (0.3 equiv), pyrene (6 equiv), MeCN, 80 °C, 36 h; (b) Excess TBACl, H$_2$O; (c) Liquid/liquid extraction/CHCl$_3$; (d) HPLC; (e) NH$_4$PF$_6$/Eluent.

moving up and/or down at independent, set rates to ensure good mixing. After the injection takes place, data collection begins simultaneously in the NMR spectrometer. Based on the area of the peaks, the quantification of each species in solution can be obtained in the presence of an internal standard.

*Coronene⊂**ExCage**·6PF$_6$.* An NMR tube was charged with 500 μL of a previously prepared solution containing coronene (0.45 mg, 1.5 μmol) and 1,5-cyclooctadiene (0.33 mg, 3.6 μmol) in DMF-d_7. The tube was inserted into the probe of the NMR spectrometer, cooled to −55 °C with the NMR cap removed. The injector system was lowered into the spectrometer and allowed to cool for 15 s. Once cooled, the **ExCage**·6PF$_6$ solution was injected (300 μL, 5.83 mM) in DMF-d_7 at a rate of 150 μL s^{-1} over 2 s. Once injected, the injector was used to mix the solution over a period of ∼8 s. The progress of the reaction was monitored by the disappearance of the CH_2 signal (6.04 ppm) for **ExCage**$^{6+}$ and the formation of the coronene signal (7.06 ppm) for coronene⊂**ExCage**·6PF$_6$ in comparison with an internal reference (1,5-cyclooctadiene, 5.43 ppm) using the ^{1}H NMR spectrometer to collect a spectrum every 36 s (parameters: at = 4.096, d1 = 0, pw = 12.2, and nt = 1).

*Pyrene⊂**ExCage**·6PF$_6$.* An NMR tube was charged with 500 μL of a previously prepared solution containing pyrene (0.30 mg, 1.5 μmol) and 1,5-cyclooctadiene (0.33 mg, 3.6 μmol) in DMF-d_7. The tube was inserted into the probe of the NMR spectrometer cooled to −55 °C with the NMR cap removed. The injector system was lowered into the spectrometer and allowed to cool for 15 s. Once cooled, the **ExCage**·6PF$_6$ solution was injected (300 μL, 5.83 mM) in DMF-d_7 at a rate of 150 μL s^{-1} over 2 s. Once injected, the injector was used to mix the solution over a period of ∼8 s. The progress of the reaction was monitored by the disappearance of the H_α and H_β signals (9.18−8.96 ppm) for **ExCage**$^{6+}$ and the formation of a H_{pyr} signal (6.27 ppm) for pyrene⊂**ExCage**·6PF$_6$ in comparison with an internal reference (1,5-cyclooctadiene, 5.43 ppm) using the ^{1}H NMR spectrometer to collect a spectrum every 5 s (parameters: at = 4.096, d1 = 0, pw = 12.2, and nt = 1).

RESULTS AND DISCUSSION

Conceptually, the replacement of a "divalent" 1,4-disubstituted benzenoid ring by a "trivalent" one that is 1,3,5-trisubstituted is analogous[28] to the replacement of two diagonally related oxygen atoms in 18-crown-6 by two trivalent nitrogen atoms in [2.2.2]cryptand.

Template-Directed Synthesis and Characterization. The synthesis (Scheme 1) of **ExCage**·6PF$_6$ starts from the previously reported[29] 1,3,5-tris(4-pyridyl)benzene (**TP**) which was alkylated in MeCN/CH_2Cl_2 (2:1) under reflux for 3 days with a 15-fold excess of 1,4-bis(bromomethyl)benzene, affording the tribromide **TB**·3PF$_6$ in 75% yield, following counterion exchange (NH$_4$PF$_6$) in MeOH. Reaction of the tribromide with another equivalent of **TP** in MeCN in the presence of 0.3 equiv of tetrabutylammonium iodide (TBAI) as a catalyst[30] for 36 h at 80 °C afforded crude **ExCage**·6Cl, following the addition of TBACl to the reaction mixture to precipitate the crude product which, after preparative reverse-phase HPLC, was precipitated from the eluent with NH$_4$PF$_6$ to give **ExCage**·6PF$_6$ in 7% yield. In the absence of the catalyst only trace amounts of **ExCage**·6PF$_6$ were isolated. However, when the reaction was repeated in the presence of the catalyst, first of all employing phenanthrene (6 equiv) as a template and then pyrene (6 equiv), the yields were much improved. In both the template-directed syntheses with TBAI present, the reaction mixtures, following the addition of TBACl, had to be subjected to continuous liquid−liquid extraction with $CHCl_3$ in order to remove the templates, prior to being subjected to preparative reverse-phase chromatography, followed by counterion exchange by adding NH$_4$PF$_6$ to the eluent. Although the use of pyrene as a template raised the yield of **ExCage**·6PF$_6$ to 45%, the template proved somewhat difficult to remove by continuous liquid−liquid extraction while phenanthrene, which was easier to extract with $CHCl_3$, resulted in a 35% yield of the final product. In the absence of the catalyst, but in the presence of the templates, the yields of the reaction, carried out at room temperature for 21 days, were considerably less, namely, 9 and 11% using phenanthrene and pyrene, respectively. In all cases, the products were characterized by high-resolution mass spectrometry and both ^{1}H and ^{13}C NMR spectroscopy. Single crystals, suitable for X-ray crystallography, were obtained by vapor diffusion of iPr$_2$O into a solution of

dx.doi.org/10.1021/ja5041557 | J. Am. Chem. Soc. 2014, 136, 10669−10682

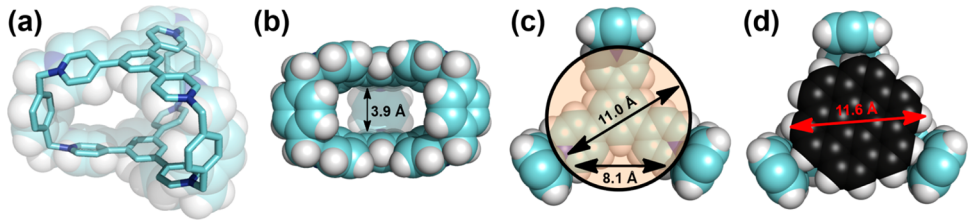

Figure 2. (a) A perspective view of a stick diagram overlaid by a space-filling representation of the X-ray crystal structure of **ExCage**$^{6+}$. (b) A side-on view of the solid-state structure of **ExCage**$^{6+}$, employing a space-filling representation and highlighting the van der Waals surface (3.9 Å) separations top-to-bottom between the two **TP** triangles. (c) A cut-away space-filling plan view of the cavity inside **ExCage**$^{6+}$, showing that the diameter (~11.0 Å) available inside the cage for the binding of a PAH is considerably larger than the maximum in-plane widths (8.1 Å) of the three identical apertures to the cage. (d) A cut-away space-filling plan view of **ExCage**$^{6+}$, illustrating the central location of coronene (black), with a minimum van der Waals diameter of 11.6 Å inside the cage's cavity. Cyan = carbon, blue = nitrogen, gray = hydrogen.

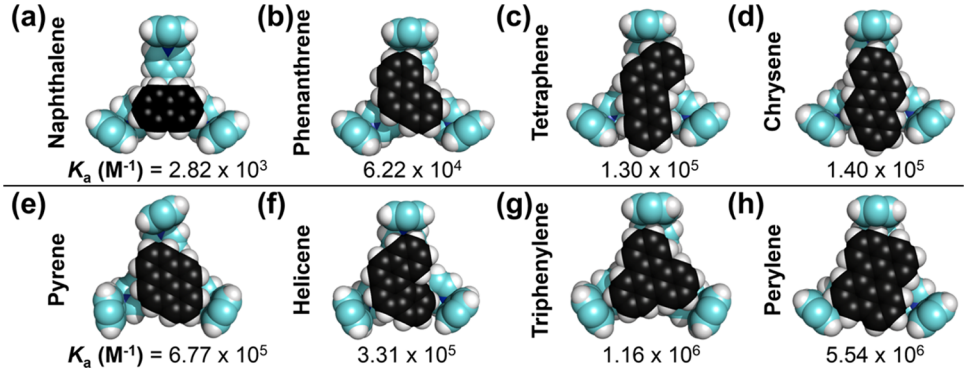

Figure 3. Cut-away space-filling plan-view representation of the solid-state superstructures of the 1:1 complexes formed between **ExCage**$^{6+}$ and (a) naphthalene, (b) phenanthrene, (c) tetraphene, (d) chrysene, (e) pyrene, (f) helicene, (g) triphenylene, and (h) perylene. Solvent molecules and counterions have been omitted for the sake of clarity. Cyan = carbon, blue = nitrogen, gray = hydrogen, black = PAH. The K_a values (M^{-1}) were determined by ITC in MeCN solutions at 25 °C.

ExCage·6PF_6 in MeCN. The solid-state structure (Figure 2a) of **ExCage**$^{6+}$ confirms that it is composed of six pyridinium units emanating from the 1, 3, and 5 positions on the two central benzenoid cores and connected together by three bridging *p*-xylylene linkers. The cage has an internal cavity depth (Figure 2b) of 3.9 Å between opposing 1,3,5-tris(4-pyridinium)benzene platforms and measures (Figure 2c) 8.1 Å between each *p*-xylylene linker, as measured by taking van der Waals radii into account. Since the former distance allows near-perfect cofacial $\pi-\pi$ stacking interactions between the host and an aromatic guest, **ExCage**$^{6+}$ is poised to bind planar π-electron-rich aromatic guests with high affinities. Furthermore, the diameter (11.0 Å) of the circular cavity inside **ExCage**$^{6+}$ exceeds (Figure 2c) that (8.1 Å) of the openings between the bridging *p*-xylylene units. We surmise that these differences in distances might impose (Figure 2d) a steric barrier to complexation and decomplexation in the case of larger aromatic guests like coronene with a minimum van der Waals radius of 11.6 Å.

CV of **ExCage**·6PF_6 in DMF shows three two-electron reductions at −0.93, −1.04, and −1.33 V, that not only match quite closely the three one-electron reductions (Figure S28) at −0.90, −1.00, and −1.34 V for the model trication obtained on methylating **TP** but also indicate a lack of electronic coupling between the two 1,3,5-tris(4-pyridinium)benzene platforms. The increasingly negative values of the potentials associated with the first, second, and third two-electron reductions establish the fact that there is some electronic coupling between the three pyridinium units within each 1,3,5-tris(4-pyridinium)benzene platform in **ExCage**$^{6+}$. In comparison[20] with **ExBox**$^{4+}$ and **Ex^{2}Box**$^{4+}$, the reduction potentials are significantly more negative, possibly because of the *meta*, rather than the *para*, substitutions of the central benzenoid cores of **ExCage**$^{6+}$. The lack of reversibility of the reduction processes in this case is a consequence of a decrease in the solubility of **ExCage**·6PF_6 that occurs with its progressive loss of charge on reduction.

Inclusion Complex Formation. PAHs—molecules which consist of two or more fused aromatic rings—are commonly found in natural crude oil deposits[31] and also arise from anthropogenic processes during the incomplete combustion of carbon-based materials.[32] The carcinogenic properties of PAHs have long been known,[33] and the pathways by which they cause mutagenesis are well documented.[34] Not only are they prevalent in the environment, but they also persist on account of their low solubilities in water. The smaller PAHs, however, such as naphthalene,[35] have a slightly higher water solubility and so are apt to leach out into waterways. Yet, despite this situation, and its implications in relation to several disease states,[36] naphthalene is produced annually on a massive scale.[37] Although numerous hosts, with affinities for PAHs, based on dispersion forces and solvophobic effects, have been reported,[38] the donor−acceptor interactions that have come into play with π-electron-deficient hosts,[39] such as in the **Ex^{n}Box** series,[20] lead to higher binding affinities for PAHs, even in organic solvents. At the outset we anticipated that the increased degree of π-electron deficiency of **ExCage**$^{6+}$, in addition to its three-dimensional bicyclic constitution, would endow it with an even higher affinity for PAHs by several orders of magnitude compared with **ExBox**$^{4+}$ and **Ex^{2}Box**$^{4+}$. There was also the expectation that **ExCage**$^{6+}$ might bind smaller PAHs like naphthalene, much more strongly than its two-dimensional counterparts.

dx.doi.org/10.1021/ja5041557 | *J. Am. Chem. Soc.* 2014, 136, 10669−10682

Table 1. K_a Values and Thermodynamic Parameters for the 1:1 Complexes Formed between ExCage·6PF$_6$ and PAH Guests in MeCN at 25 °C

PAH	$\pi\ e^-$	K_a (10^3 M^{-1})	ΔH (kcal mol^{-1})	ΔS (cal mol^{-1}K^{-1})	ΔG^0 (kcal mol^{-1})
naphthalene	10	2.82 ± 0.7	−3.02 ± 0.59	+5.60 ± 1.65	−4.71 ± 0.15
phenanthrene	14	62.2 ± 2.6	−9.07 ± 0.08	−8.49 ± 2.56	−5.34 ± 0.15
tetraphene	18	130 ± 25	−9.53 ± 0.26	−8.78 ± 1.05	−6.97 ± 0.11
chrysene	18	140 ± 7.0	−8.93 ± 0.12	−6.42 ± 0.51	−7.02 ± 0.03
pyrene	16	677 ± 97	−10.82 ± 0.11	−9.10 ± 1.34	−7.95 ± 0.09
helicene	18	331 ± 30	−12.52 ± 0.75	−1680 ± 2.35	−7.53 ± 0.05
triphenylene	18	1160 ± 90	−13.4 ± 0.03	−16.5 ± 0.82	−8.27 ± 0.04
perylene	20	5540 ± 20	−13.1 ± 0.1	−12.9 ± 0.01	−9.20 ± 0.01
coronene[a]	24	30000[b]	N/A	N/A	N/A

[a]The binding constant (K_a value) and thermodynamic parameters for coronene could not be obtained by ITC on account of its insolubility in MeCN. [b]The K_a value for coronene is an estimate, based on a linear regression of the binding constants plotted against the number of n-electrons in naphthalene, phenanthrene, pyrene, triphenylene, and perylene. See the red diamond in Figure 3.

The inclusion complexes formed between **ExCage**$^{6+}$ and various PAHs were explored both in the solid state and in solution. Ranging from two to seven fused benzenoid rings, the crystalline complexes formed (Figure 3) between **ExCage**$^{6+}$ and naphthalene, phenanthrene, tetraphene, chrysene, pyrene, helicene, triphenylene, and perylene in addition to coronene (Figure 2d) were isolated. It should be noted that, regardless of the excess of guest employed—ranging from 2 to 40 equiv in the generation of single crystals by vapor diffusion of iPr$_2$O into MeCN solutions of the host–guest mixtures—the results invariably yield crystals with a 1:1 stoichiometry between host and guest. The relative translational positioning of the smaller guests (e.g., naphthalene and phenanthrene) inside the host and the relative rotational location of the larger guests (e.g., triphenylene and perylene) with respect to the pyridinium units of **ExCage**$^{6+}$ appears to be such that the PAHs align themselves in register with the maximum number of binding sites, allowing for the optimal interactions between the π-electron-rich guests and the π-electron-deficient portions of the host. This observation was confirmed by UV–vis spectrophotometric analysis of the inclusion complexes in MeCN, which reveal the presence of charge-transfer bands (Figure S29b) in the case of every PAH guest investigated. It follows that the favorable binding forces can be considered to be comprised of charge-transfer interactions, in addition to stabilizing π–π stacking attractions and [C–H···π] interactions involving the bridging p-xylylene units.

In order to quantify the extent of the binding between the PAH guests and **ExCage**$^{6+}$, ITC was performed in MeCN (Table 1 and Figure 3) or DMF (Table 3 and Figure S19) to determine the binding constants and thermodynamic parameters for the 1:1 complexes formed between **ExCage**·6PF$_6$ and the series of PAH guests in MeCN (or DMF) at 25 °C. The complexation strengths follow an approximately linear trend (Figure 4) of increasing K_a values (on a logarithmic scale) with the increasing number of π-electrons in the guests. Tetraphene, chrysene, and helicene are outliers in the context of this linear relationship, presumably because of the curtailed presence of stabilizing interactions between these PAH guests and **ExCage**$^{6+}$. In the case of tetraphene and chrysene, partial π–π stabilization is achieved only when a portion of the PAH guest molecule is not located inside **ExCage**$^{6+}$, while the distortion from nonplanarity in the case of helicene disrupts the cofacial π–π interactions inside the host. Although a K_a value for coronene could not be obtained experimentally on account of its insolubility in both MeCN and DMF, estimated binding constants in the region of 3×10^8 M^{-1} in MeCN and 7×10^7 M^{-1} in DMF can be surmised on the basis of the linear relationship illustrated in Figures 4 and S19, respectively. While only an estimate, these predicted K_a values are supported by the fact that coronene does not undergo exchange (Figure S26d) on the ^{1}H NMR time scale with free cage molecules in DMF-d_7 solution at 145 °C.

Rebek's 55% rule states[40] that the binding of guests within a host, assuming only the weakest of interactions therein, is expected to be favorable when the guest occupies approximately 55% of the host volume. By Rebek's own admission, "it may be difficult to judge binding capabilities based on volume considerations alone" when "either large holes in the structures or an opening to the exterior", as in the case of **ExCage**$^{6+}$, "do not often allow a precise definition of an internal molecular cavity". Clearly, we have to make some wholesale assumptions in estimating the internal volume of **ExCage**$^{6+}$. Thus, in order to compare the volume occupancy of the PAHs bound within the cavity of **ExCage**$^{6+}$ to Rebek's formula for molecular recognition in the liquid state, each inclusion complex has been analyzed (Table S3) in the solid state using a rough-and-ready overlap model to obtain an estimate of percent occupancies of the PAH guests within the **ExCage**$^{6+}$ cavity. The guest-accessible volumes of **ExCage**$^{6+}$ were assumed[41] to be the same, i.e., 213 ± 7 Å^3, for the binding of each PAH guest. When this volume was used to calculate the percent occupancies of each PAH guest within **ExCage**$^{6+}$, we obtained values of 53% for naphthalene, 66% for

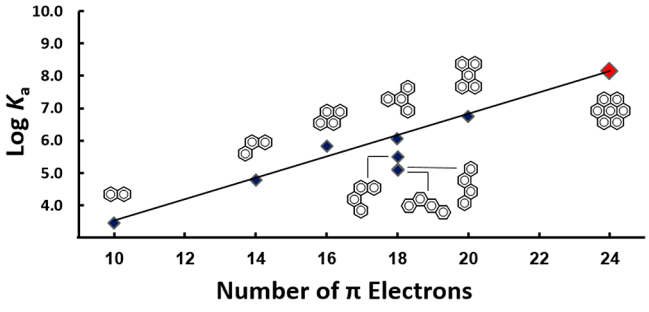

Figure 4. A linear plot of the binding affinities (log Ka's) in MeCN between **ExCage**$^{6+}$ and the number of π-electrons present in the eight PAHs, introduced in the previous figure, plus coronene (see the red diamond whose location is the result of a linear regression) for which there is no experimentally derived K_a value on account of its lack of solubility in MeCN. Note that helicene, whose structure deviates from planarity, and tetraphene and chrysene, which have elongated constitutions, lie below the line.

dx.doi.org/10.1021/ja5041557 | J. Am. Chem. Soc. 2014, 136, 10669–10682

phenanthrene, 67% for tetraphene, 69% for chrysene, 70% for pyrene, 89% for helicene, 87% for triphenylene, 83% for perylene, and 90% for coronene. Only the smallest of the PAHs, namely, naphthalene, occupies nearly 55% of the **ExCage**$^{6+}$ cavity. In agreement with Rebek's findings, naphthalene exhibits (Table 1) a relatively low enthalpy of binding which is offset to some extent by a favorable (positive) entropy of binding. By contrast, the remaining PAHs experience increasing enthalpies of binding commensurate with the introduction of more and more molecular recognition on account of increasing face-to-face and edge-to-face $\pi-\pi$ stacking interactions. The consequences are that, as the K_a values increase by two orders of magnitude, the contribution from the enthalpies of binding become larger and larger and that from the entropies of binding become less and less, while the percent volume occupancies of the PAHs approach 90%. This line of reasoning leads us to propose that the binding constant ($K_a > 3 \times 10^8$ M^{-1}) we obtained for coronene with **ExCage**$^{6+}$, based (Figure 4) on a linear relationship between log K_a and the number of π-electrons, amounts to a reasonable piece of speculation.

The trend of increasing K_a values (on a logarithmic scale) with the increasing number of π-electrons in the guests is consistent with that observed recently[20] in the **ExBox** series of cyclophanes. However, although the order from weak-to-strong binding of PAHs is similar to that exhibited by **ExBox**$^{4+}$, the K_a values for the comparable 1:1 complexes with **ExCage**$^{6+}$ are one-to-two orders of magnitude higher. This increase in binding strength becomes especially noticeable when, in contrast with its two-dimensional **ExBox**$^{4+}$ counterparts, **ExCage**$^{6+}$ is able to bind the smallest PAHs, i.e., naphthalene with a K_a value >10^3 M^{-1} in MeCN. In order to be sure that the stoichiometry between **ExCage**$^{6+}$ and naphthalene in solution is consistent with that observed in the solid-state superstructure, a Job plot (Figure 5) was carried out

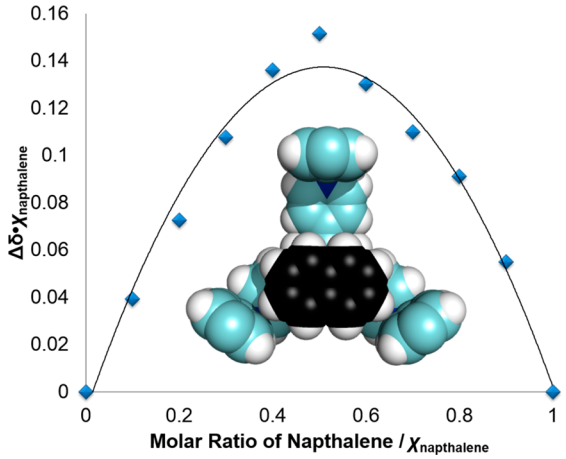

Figure 5. A Job plot for the inclusion complex formed between **ExCage**$^{6+}$ and naphthalene in CD_3CN at room temperature showing that, in solution, the cage binds the smallest guest investigated in a 1:1 ratio.

and shown to confirm the 1:1 stoichiometry of the complex in CD_3CN solution. In order to demonstrate the potential of **ExCage**$^{6+}$ to bind with very small PAHs, we tested its ability to sequester naphthalene from water. Starting (Figure 6) with a saturated aqueous solution (~31 mg L^{-1}) of naphthalene[42] containing trace amounts of hexane-2,5-dione as a nonbinding standard, **ExCage**$^{6+}$ (1.2 equiv) as its water-insoluble hexafluorophosphate salt, was added and the heterogeneous mixture was

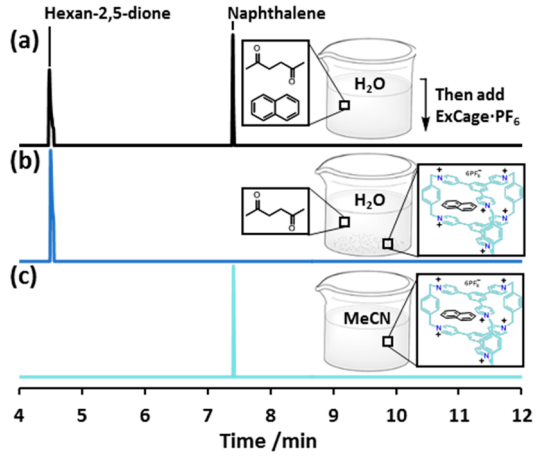

Figure 6. GC/MS traces (a) showing an aqueous satd solution of naphthalene containing a small amount of hexane-2,5-dione as an internal standard and also (b) after adding **ExCage**$^{6+}$ as its insoluble PF_6^- salt, sonicating, filtering off the solid, and injecting the solution into the GC/MS to reveal a trace containing only the internal standard, i.e., all the naphthalene has been scavenged from the satd aqueous solution. A GC/MS trace showing (c) the result when the solid that was filtered off (above) is dissolved in MeCN and injected into the GC/MS, i.e., the peak for the naphthalene reappears and the internal standard is absent.

subjected to sonication for 30 min. The solid was filtered off and the solute was examined by GC/MS. The chromatogram (Figure 6b) shows the complete removal of the naphthalene from the water by **ExCage**·6PF_6. Furthermore, upon dissolution of the 1:1 complex between naphthalene and **ExCage**·6PF_6 in MeCN, free naphthalene was observed (Figure 6c) in the solution by GC/MS.

Kinetics of Complexation and Decomplexation. The fact that the three equivalent apertures between the *p*-xylylene linkers in **ExCage**$^{6+}$ are smaller (8.1 Å) than its internal diameter (11.0 Å) suggests that coronene, with a maximum width of 11.9 Å (and minimum width of 11.6 Å), in van der Waals radii, might be confronted with a measurable kinetic barrier when entering the cage. Given these steric considerations,[43] we decided to probe the energy barriers to complexation and decomplexation using (i) rapid injection ^{1}H NMR (RI-NMR) spectroscopy and (ii) dynamic ^{1}H NMR (VT-NMR) spectroscopy, respectively.

RI-NMR Spectroscopy. We carried out our initial investigations, designed to probe the relative rates of complexation of pyrene and coronene by **ExCage**·6PF_6 in DMF-d_7 at −55 °C. A slight excess of the host (1.7 μmol) in 300 μL was injected into a solution of pyrene (1.5 μmol) in 500 μL and complexation was monitored (Figure 7a) at 5 s intervals by following (i) the disappearance of the resonances at 9.71, 9.15, 9.04, and 6.05 ppm for H_α, H_γ, H_β, and the CH_2 protons, respectively, in the free cage, and (ii) the appearance of resonances at 9.66, 6.29, 6.20, and 6.14 ppm for H_α', pyrene (two of the resonances overlapping at 6.20, with the third at 6.29 ppm), and the CH_2' protons, respectively, for the 1:1 complex. In the case of coronene, a slight excess of **ExCage**·6PF_6 (1.7 μmol) in 300 μL was injected into a solution of coronene (1.5 μmol) in 500 μL and the complexation by **ExCage**$^{6+}$ was monitored (Figure 7b) at 36 s intervals by following (i) the disappearance of resonances at 9.69 and 6.05 ppm for H_α and the CH_2 protons, respectively, in the free cage and (ii) the appearance of resonances at 9.58, 7.06, and 6.21 ppm for H_α', coronene, and the CH_2' protons, respectively, in the 1:1 complex. By duplicating the experimental procedures for the

dx.doi.org/10.1021/ja5041557 | J. Am. Chem. Soc. 2014, 136, 10669−10682

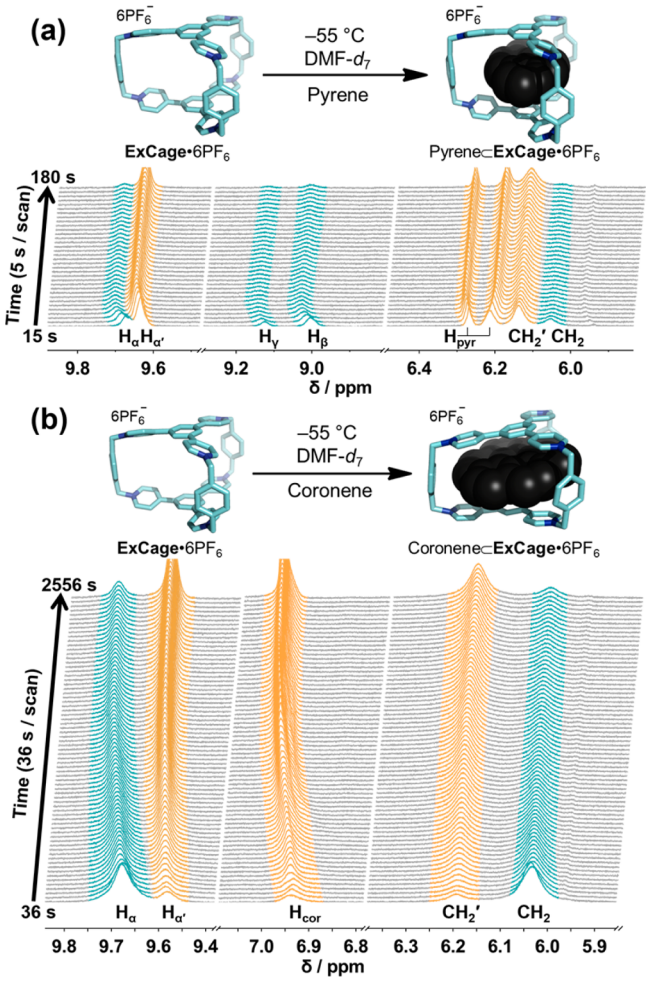

Figure 7. (a) Stacked ^{1}H NMR spectra (from 5.8 to 6.5, 8.8 to 9.3, and 9.5 to 9.9 ppm) of 1 equiv of pyrene in DMF-d_7 from time 15 to 180 s following the injection of ∼1.15 equiv of **ExCage**·6PF$_6$ in DMF-d_7 at −55 °C. The disappearance of resonances for the host, associated with the protons, H$_\alpha$, H$_\beta$, H$_\gamma$, and CH$_2$ (highlighted in cyan) and the appearance of the resonances, H$_\alpha$′, H$_{pyr}$, and CH$_2$′ (highlighted in orange), over the course of 20 s, indicates the rapid formation of the pyrene⊂**ExCage**·6PF$_6$, 1:1 complex. (b) Stacked ^{1}H NMR spectra (from 5.9 to 6.4, 6.8 to 7.2, and 9.4 to 9.9 ppm) of 1 equiv of coronene in DMF-d_7 from time 36 to 2556 s, following the injection of ∼1.15 equiv of **ExCage**·6PF$_6$ in DMF-d_7 at −55 °C. The disappearance of resonances for the host, associated with the protons, H$_\alpha$, and CH$_2$ (highlighted in cyan), and the appearance of resonances, H$_\alpha$′, H$_{cor}$, and CH$_2$′ (highlighted in orange), indicates the relatively slow formation of the coronene⊂**ExCage**·6PF$_6$, 1:1 complex.

binding of (i) pyrene and (ii) coronene, the identical concentrations and temperature allows a direct comparison of the association rates of the two data sets, such that the relative intensities of the disappearing and appearing resonances reveal that pyrene enters the cavity of **ExCage**$^{6+}$ much faster than does coronene. The association of pyrene was complete after the collection of six data points, i.e., in <30 s. By contrast, coronene takes more than 40 min to associate with **ExCage**$^{6+}$, exhibiting second-order kinetics where the rate constant, $k = 5.95 \times 10^{-4}$ mM^{-1} s^{-1}. The kinetic data (Figure S27a−d) confirm that a small barrier to complexation does exist and follows size dependence, validating a "gating" effect, which has been observed in both synthetic[44] and biological[45] receptors previously.

VT-NMR Spectroscopy. The ^{1}H NMR spectra of a 2:1 ratio of **ExCage**·6PF$_6$ and each of the four (phenanthrene, pyrene, triphenylene, and coronene) PAHs were recorded (Figure 8 and Figure S26a-d) separately at temperatures ranging from −55 to +75 (phenanthrene), to +95 (pyrene), and to +145 °C (triphenylene and coronene) in DMF-d_7. In general, the exchange of protons H$_\beta$, H$_\gamma$, and Ph in the uncomplexed (free) **ExCage**$^{6+}$ with those, H$_\beta$′, H$_\gamma$′, and Ph′ in the complexed **ExCage**$^{6+}$ is associated with extensive overlapping and broadening in the ^{1}H NMR spectra as a result of the fast exchange of the pairs of probe protons at higher temperatures (resulting in well-resolved "averaged" spectra) and their slow exchange at lower temperatures where the resonances for the pairs of probe protons each separate out into two well-resolved peaks. In the vicinity of the coalescence temperatures, where the line shapes become so broad they almost merge into the baseline, we can identify (Table 2) an approximate coalescence temperature (T_c) of −15, +25, +65, and > +145 °C for the pairs of exchanging protons in phenanthrene, pyrene, triphenylene, and coronene, respectively. The VT-NMR spectra for phenanthrene (Figure 8a) and triphenylene (Figure 8b) provide two good representative examples of the spectroscopic data we have collected. In the case of phenanthrene (Figure 8a), at −55 °C, the signal for the H$_\gamma$ protons at 9.14 ppm and that for the H$_\gamma$′ at 8.14 ppm coalesce to produce one resonance at 8.54 ppm at +75 °C, while the resonance for the H$_\beta$ protons at 9.03 ppm and that for the H$_\beta$′ protons at 8.27 ppm coalesce to 8.62 ppm. In the example of triphenylene (Figure 8b), the resonances for the H$_\gamma$ and H$_\beta$ protons in the free **ExCage**$^{6+}$ at −55 °C also have chemical shifts of 9.14 and 9.03 ppm, respectively, while the signals for the H$_\gamma$′ and H$_\beta$′ protons resonate at 8.08 and 8.57 ppm, respectively. The

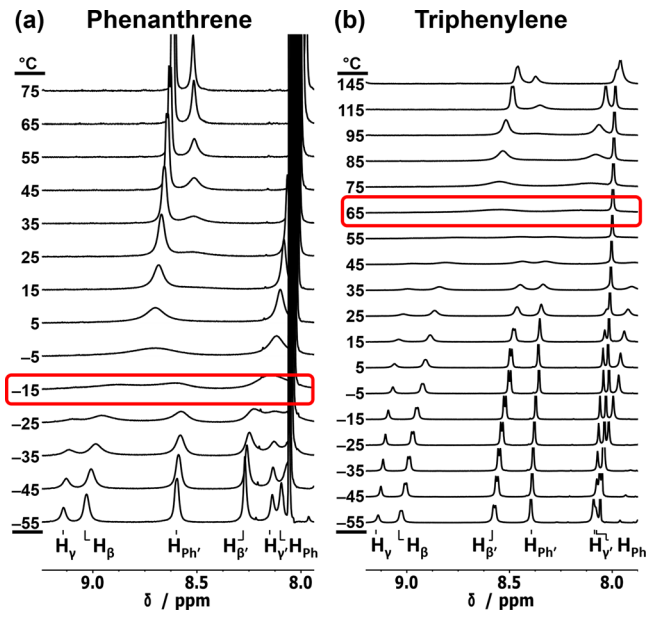

Figure 8. VT ^{1}H NMR spectroscopic studies performed at 600 MHz showing (a) stacked ^{1}H NMR spectra (from 8.0 to 9.2 ppm) recorded for a mixture consisting of 2 equiv of **ExCage**·6PF$_6$ and 1 equiv of phenanthrene over a range of temperatures (−55 to 75 °C) in DMF-d_7 with a coalescence temperature (T_c) of approximately −15 °C (boxed in red). (b) Stacked ^{1}H NMR spectra (from 7.9 to 9.2 ppm) recorded for a mixture consisting of 2 equiv of **ExCage**·6PF$_6$ and 1 equiv of triphenylene over a range of temperatures (−55 to 145 °C) in DMF-d_7 with a T_c of approximately 65 °C (boxed in red).

dx.doi.org/10.1021/ja5041557 | J. Am. Chem. Soc. 2014, 136, 10669−10682

Table 2. VT ^{1}H NMR Spectroscopic Data for 2:1 Mixtures of ExCage·6PF$_6$ and Selected PAHs in DMF-d_7 Depicting the Changes in Chemical Shifts of Probe Proton Signals along with the Calculated Rate Constants and Barriers to Decomplexation

	ΔV_{max} (Hz)[a]				k_c (Hz)[c]			$\Delta G_c^{\ddagger}$ (kcal mol^{-1})[e]		
PAH	H_β/H_β'	H_Y/H_Y'	H_{Ph}/H_{Ph}'	T_c (°C)[b]	H_β/H_β'	H_Y/H_Y'	H_{Ph}/H_{Ph}'	H_β/H_β'[d]	H_Y/H_Y'	H_{Ph}/H_{Ph}'
phenanthrene	259	602	105	−15	580	1300	230	11.8	11.4	12.2
pyrene	334	821	127	+25	470	1800	280	13.8	13.0	14.1
triphenylene	279	636	184	+65	620	1400	410	15.6	15.0	15.8
coronene	661	1399	358	>+145	1500	3100	800	>18.7[f]	>18.1[f]	>19.2[f]

[a]The maximum change in chemical shift between the signals for the exchanging probe protons (as assigned in Scheme 1) in the empty **ExCage**$^{6+}$ and in the PAH⊂**ExCage**$^{6+}$ complexes. [b]On account of the close proximity of signals with significant line broadening, it was not possible to determine the exact coalescence temperatures for individual signals. [c]The rate constant, k_c, at coalescence was determined using $k_c = \pi\Delta\nu/\sqrt{2}$, where $\Delta\nu$ is the limiting chemical shift differences in Hz at temperatures below T_c for the probe protons undergoing exchange. The differences in k_c that arise from using a single coalescence temperature for a selected PAH result in negligible differences in the calculated $\Delta G_c^{\ddagger}$ values. [d]The signal for the β protons was selected because of ease of analysis. [e]Values were calculated using the Eyring equation, $\Delta G_c^{\ddagger} = -RT_c\ln(k_c\hbar/k_BT_c)$, in which R is the gas constant, T_c is the temperature at coalescence, k_c is the rate constant, $\hbar$ is Planck's constant, and k_B is Boltzmann's constant. [f]Even at 145 °C, the highest temperature at which spectra were recorded, coalescence of the resonances for these pairs of probe protons was not observed.

Table 3. Thermodynamic Parameters Based on ITC Data in DMF and VT ^{1}H NMR Spectroscopy in DMF-d_7 for Selected PAH⊂ExCage^{6+} Complexes Showing the Free Energies of Complexation (ΔG^0, ITC), the Barriers to Dissociation ($\Delta G_d^{\ddagger}$, VT ^{1}H NMR), and the Calculated Barriers to Association ($\Delta G_a^{\ddagger}$)

PAH[a]	K_a (M^{-1})	ΔH (kcal mol^{-1})	ΔS (cal mol^{-1} K^{-1})	ΔG^0 (kcal mol^{-1})	$\Delta G_d^{\ddagger}$ (kcal mol^{-1})[d]	$\Delta G_a^{\ddagger}$ (kcal mol^{-1})
phenanthrene	1.3×10^4	−6.37	−2.59	−5.59	11.8	6.21
pyrene	$1.12 \pm 0.12 \times 10^5$	−6.82 ± 0.05	0.22 ± 0.13	−6.88 ± 0.05	13.6	6.72
triphenylene	$6.75 \pm 0.12 \times 10^5$	−11.2 ± 0.13	−10.9 ± 0.38	−7.95 ± 0.13	15.5	7.55
perylene[b]	$1.79 \pm 0.15 \times 10^6$	−9.42 ± 0.60	−3.01 ± 2.17	−8.52 ± 0.65	–	–
coronene[c]	(6.7×10^7)	–	–	(−10.7)	>18.7[e]	(>8.0)

[a]Samples run in triplicate. [b]Data from a single experiment. [c]The low solubility of coronene prevented the determination of a binding constant with **ExCage**$^{6+}$ by ITC and host−guest exchange was too slow on the ^{1}H NMR time-scale at room temperature for a ^{1}H NMR titration experiment. [d]Values were determined by VT ^{1}H NMR spectroscopy in DMF-d_7 from −55 to 145 °C. The free energy of activation at the coalescence temperature ($\Delta G_c^{\ddagger}$) is equated with the barrier to dissociation ($\Delta G_d^{\ddagger}$). [e]No exchange was detected at the upper temperature limit (145 °C) for DMF-d_7, by VT ^{1}H NMR spectroscopy. Values in parentheses are approximate based on a linear regression of the log K_a vs PAH electron count plot for phenanthrene, pyrene, triphenylene, and perylene. See Figure S19.

resonances for these two pairs of protons coalesce to 8.37 and 8.46 ppm at +145 °C, respectively. The limiting chemical shifts ($\Delta\nu$ values in Hz) for the particular pairs of protons (Table 2) can then be employed to calculate the rate constants (k_c) at the coalescence temperature (T_c) from whence $\Delta G_c^{\ddagger}$, which corresponds to the free energies of activation for decomplexation, can be calculated (Table 2) using the Eyring equation. The average $\Delta G_c^{\ddagger}$ values (Table 3) for phenanthrene, pyrene, triphenylene, and coronene, which are 11.8, 13.6, 15.5, and >18.7 kcal mol^{-1}, can be equated with the free energy barriers for dissociation, $\Delta G_d^{\ddagger}$. From the free energies of binding (ΔG^0), obtained from ITC, and $\Delta G_d^{\ddagger}$ values, obtained from VT-NMR, the energy barriers for association ($\Delta G_a^{\ddagger}$) were determined (Table 3) to be 6.21, 6.72, and 7.55 kcal mol^{-1} for phenanthrene, pyrene and triphenylene, respectively. Using the estimated values for ΔG^0 for coronene in DMF (−10.7 kcal mol^{-1}) and the lower limit of $\Delta G_d^{\ddagger}$ (18.7 kcal mol^{-1}), we can estimate $\Delta G_a^{\ddagger}$ to be >8.0 kcal mol^{-1}, corroborating the data obtained from the RI-NMR spectroscopy.

CONCLUSIONS

The macrobicyclic effect[6,7] becomes apparent immediately on drawing comparisons (Table 4) between the magnitudes of the association constants (K_a values) for the binding of the PAHs measured in acetonitrile and their derived ΔG^0 values on going from the "two-dimensional" **ExBox**$^{4+}$ to the "three-dimensional" **ExCage**$^{6+}$. Not only is there a rise (in K_a values) on going from left to right across Table 4 (from **ExBox**$^{4+}$ to **ExCage**$^{6+}$) of one-to-two orders of magnitude for each of the PAHs investigated, but both **ExBox**$^{4+}$ and **ExCage**$^{6+}$ gain more than two orders of magnitude in their association constants in going down the list of K_a values from phenanthrene to perylene as the π-electron count increases. The trigonal disposition of the two-times-three (six) electron-deficient pyridinium binding units of **ExCage**$^{6+}$ provides a substantial increase in the strength of the binding interactions with pyrene, helicene, triphenylene, and perylene, which have ΔG^0 values of −7.95, −7.53, −8.27, and −9.20 kcal mol^{-1}, respectively. These guests all have the ability to interact simultaneously with all three binding pockets in **ExCage**$^{6+}$. It is significant that the binding free energies of these four guests experience substantial costs in entropy (ΔS = −9.10, −16.8, −16.5, and −12.9 cal mol^{-1} K^{-1}) that goes some way toward negating their large ΔH values of −10.8, −12.5, −13.4, and −13.1 kcal mol^{-1}, respectively. It is noteworthy that all four of these 1:1 complexes are highly ordered supramolecular entities, in contrast to phenanthrene, tetraphene, and chrysene, all of which can only bind two pockets simultaneously, yet can move inside the cage and so interact with different pairs of pockets. These less well-ordered supramolecular entities exhibit smaller binding enthalpies (ΔH = −9.07, −9.53, −8.93 kcal mol^{-1}, respectively), while witnessing reduced costs in their entropies of binding (ΔS = −8.49, −8.78, and −6.42 cal mol^{-1} K^{-1}, respectively), leading to ΔG^0 values of −5.34, −6.97, and −7.02 kcal mol^{-1}, respectively.[46] The differences ($\Delta\Delta G^0$ = 1.06, 2.94, 2.43, 2.70, 2.41, 2.42, and 2.46 kcal mol^{-1}) in the ΔG^0 values for **ExBox**$^{4+}$ and **ExCage**$^{6+}$, which are listed in Table 4 from phenanthrene[47] down to perylene, provide a quantitative measure of the macrobicyclic effect. It comes to us as no surprise that the

dx.doi.org/10.1021/ja5041557 | J. Am. Chem. Soc. 2014, 136, 10669−10682

Table 4. Direct Comparison of the K_a and ΔG^0 Values for Different PAH⊂ExBox^{4+a} and PAH⊂ExCage^{6+} Complexes in MeCN at 25 °C

		K_a (10^3 M^{-1})		ΔG^0 (kcal mol^{-1})		
PAH	π e^-	**ExBox**$^{4+a}$	**ExCage**$^{6+}$	**ExBox**$^{4+a}$	**ExCage**$^{6+}$	$\Delta\Delta G^0$ (kcal mol^{-1})^b
naphthalene	10	N/A	2.82 ± 0.7	N/A	−4.71 ± 0.15	N/A
phenanthrene	14	1.38 ± 0.02	62.2 ± 2.6	−4.28 ± 0.01	−5.34 ± 0.15	1.06
tetraphene	18	0.91 ± 0.01	130 ± 25	−4.03 ± 0.01	−6.97 ± 0.11	2.94
chrysene	18	2.32 ± 0.15	140 ± 7	−4.59 ± 0.04	−7.02 ± 0.03	2.43
pyrene	16	7.16 ± 0.50	677 ± 97	−5.25 ± 0.04	−7.95 ± 0.09	2.70
helicene	18	5.71 ± 0.05	331 ± 30	−5.12 ± 0.01	−7.53 ± 0.05	2.41
triphenylene	18	19.7 ± 5.0	1160 ± 90	−5.85 ± 0.15	−8.27 ± 0.04	2.42
perylene	20	88.1 ± 67	5540 ± 20	−6.74 ± 0.45	−9.20 ± 0.01	2.46
coronene	24	N/A	30000^c	N/A	N/A	N/A

^{a}See ref 20a. ^{b}The difference between the ΔG^0 for **ExBox**$^{4+}$ and **ExCage**$^{6+}$ complexed with a particular host. ^{c}As estimated from data presented in Table 1.

binding ($\Delta G^0 = -4.71$ kcal mol^{-1}) of naphthalene in **ExCage**$^{6+}$ is both enthalpically ($\Delta H = -3.02$ kcal mol^{-1}) and entropically ($\Delta S = +5.60$ cal mol^{-1} K^{-1}) driven, reflecting the fact that, although it can access two binding pockets, it is competing with an included MeCN molecule inside what is presumably a highly disordered "ternary complex". Given its favorable entropy of binding, naphthalene, with a volume occupany of 53%, proves to be in good agreement with Rebek's 55% rule. The remaining guests, which all occupy a significantly larger portion of the host, exhibit higher binding on account of the ever-increasing degree of engineered molecular recognition in **ExCage**$^{6+}$.

Cram[48] has defined (Figure 9) intrinsic binding as the free energy of complexation (ΔG^0) of a guest by a host and constrictive binding as the free energy of activation ($\Delta G_a^{\ddagger}$) for that complexation. It follows that the free energy of activation ($\Delta G_d^{\ddagger}$) for decomplexation is equal to the sum of the intrinsic and constrictive binding, namely $\Delta G_a^{\ddagger} + \Delta G^0 = \Delta G_d^{\ddagger}$. In a comparison with hemicarcerands binding small molecules like butan-2-one, the $\Delta G_d^{\ddagger}$ and $\Delta G_a^{\ddagger}$ values (Table 2) are considerably less for **ExCage**$^{6+}$ in its binding of PAH guests, reflecting the fact their kinetics of association and dissociation are both very fast. By contrast, the binding energies (ΔG^0) are much larger in the case of **ExCage**$^{6+}$ on account of its built-in molecular recognition for π-electron-rich guests, created by three trigonally disposed pyridinium binding pockets. All-organic cages with built-in recognition sites on their inner (concave) surfaces, which act cooperatively to complex strongly with all-organic guests are, as of yet, few and far between in comparison with hosts containing convergent metal−ligand binding sites. It would seem to us that there is a need to identify and design more cage-like hosts endowed with convergent molecular recognition sites that act cooperatively in their binding of specific all-organic guests.

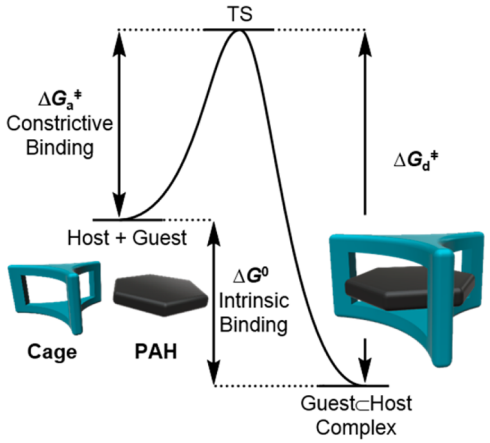

Figure 9. Reaction coordinate diagram for the complexation/decomplexation of a guest (PAH) inside a generic host (cage) illustrating the relationship between the $\Delta G_a^{\ddagger}$ (free energy of association or constrictive binding energy), the $\Delta G_d^{\ddagger}$ (free energy of dissociation), and the ΔG^0 (ground-state free energy or intrinsic binding energy).

■ ASSOCIATED CONTENT

Supporting Information

Detailed synthetic procedures and characterization (NMR and HRMS) data for all compounds, crystallographic and spectroscopic (NMR, VT-NMR, RI-NMR) characterization for **ExCage**·6PF$_6$ and inclusion complexes of **ExCage**·6PF$_6$ with naphthalene, phenanthrene, tetraphene, chrysene, pyrene, helicene, triphenylene, perylene, and coronene, along with their respective binding data (ITC), and UV−vis analysis. This material is available free of charge via the Internet at http://pubs.acs.org.

■ AUTHOR INFORMATION

Corresponding Author

stoddart@northwestern.edu

Notes

The authors declare no competing financial interest.

■ ACKNOWLEDGMENTS

The data reported in this paper are tabulated in the Supporting Information and the crystallographic parameters of each single crystal were deposited into the Cambridge Crystallographic Data Centre (CCDC). This research is part (Project no. 94-938) of the Joint Center of Excellence in Integrated Nano-Systems (JCIN) at King Abdul-Aziz City for Science and Technology (KACST) and Northwestern University (NU). The authors would like to thank both KACST and NU for their continued support of this research. A.A.T. and S.E.D. thank the National Science Foundation (NSF CHE1012663 and CHE1151566) for generous financial support. E.J.D. and N.L.S. are supported by a Graduate Research Fellowship (GRF) from the National Science Foundation (NSF). J.C.B. was supported by a National Defense Science and Engineering Graduate Fellowship (32 CFR 168a) from the Department of Defense (DoD) and gratefully acknowledges support from the Ryan Fellowship and the

Northwestern University International Institute for Nanotechnology. M.J. gratefully acknowledges The Netherlands Organization for Scientific Research (NWO) and the Marie Curie Cofund Action (Rubicon Fellowship). A.K.B. acknowledges Fulbright New Zealand for a Fulbright Graduate Award and the New Zealand Federation of Graduate Women for a Postgraduate Fellowship Award.

REFERENCES

(1) Pedersen, C. J. *Angew. Chem., Int. Ed. Engl.* **1988**, *27*, 1021.
(2) (a) Pedersen, C. J. *Aldrichimica Acta* **1971**, *4*, 1. (b) Schroeder, H. E.; Pedersen, C. J. *Pure Appl. Chem.* **1988**, *60*, 445.
(3) Pedersen, C. J. *J. Am. Chem. Soc.* **1967**, *89*, 7017.
(4) (a) Lehn, J.-M. *Angew. Chem., Int. Ed. Engl.* **1988**, *27*, 89. (b) Lehn, J.-M. *Supramolecular Chemistry: Concepts and Perspectives*; Wiley VCH: Weinheim, Germany, 1995.
(5) (a) Simmons, H. E.; Park, C. H. *J. Am. Chem. Soc.* **1968**, *90*, 2428. (b) Park, C. H.; Simmons, H. E. *J. Am. Chem. Soc.* **1968**, *90*, 2429. (c) Park, C. H.; Simmons, H. E. *J. Am. Chem. Soc.* **1968**, *90*, 2431.
(6) (a) Dietrich, B.; Lehn, J.-M.; Sauvage, J.-P. *Tetrahedron Lett.* **1969**, 2885. (b) Dietrich, B.; Lehn, J.-M.; Sauvage, J.-P.; Blanzat, J. *Tetrahedron* **1973**, *29*, 1629.
(7) (a) Dietrich, B.; Lehn, J.-M.; Sauvage, J.-P. *Tetrahedron Lett.* **1969**, 2889. (b) Dietrich, B.; Lehn, J.-M.; Sauvage, J.-P. *Tetrahedron* **1973**, *29*, 1647. (c) Huang, R. H.; Faber, M. K.; Moeggenborg, K. J.; Ward, D. L.; Dye, J. L. *Nature* **1988**, *331*, 599. (d) von Hänisch, C.; Hampe, O.; Weigend, F.; Stahl, S. *Angew. Chem., Int. Ed.* **2007**, *46*, 4775. (e) Rupar, P. A.; Staroverov, V. N.; Baines, K. M. *Science* **2008**, *322*, 1360. (f) Hao, H.-G.; Zheng, X.-D.; Lu, T.-B. *Angew. Chem., Int. Ed.* **2010**, *49*, 8148. (g) Lopez, N.; Graham, D. J.; McGuire, R.; Alliger, G. E.; Shao-Horn, Y.; Cummins, C. C.; Nocera, D. G. *Science* **2012**, *335*, 450. (h) Wei, P.; Xia, B.; Zhang, Y.; Yu, Y.; Yan, X. *Chem. Commun.* **2014**, *50*, 3973.
(8) (a) Cram, D. J.; Kaneda, T.; Helgeson, R. C.; Brown, S. B.; Knobler, C. B.; Maverick, E.; Trueblood, K. N. *J. Am. Chem. Soc.* **1985**, *107*, 3645. (b) Cram, D. J.; Lein, G. M. *J. Am. Chem. Soc.* **1985**, *107*, 3657. (c) Bryant, J. A.; Ho, S. P.; Knobler, C. B.; Cram, D. J. *J. Am. Chem. Soc.* **1990**, *112*, 5837. (d) Mitjaville, J.; Caminade, A.-M.; Mathieu, R.; Majoral, J.-P. *J. Am. Chem. Soc.* **1994**, *116*, 5007. (e) Yi, H.-P.; Wu, J.; Ding, K.-L.; Jiang, X.-K.; Li, Z.-T. *J. Org. Chem.* **2007**, *72*, 870. (f) Skowronek, P.; Gawronski, J. *Org. Lett.* **2008**, *10*, 4755. (g) Giri, N.; Davidson, C. E.; Melaugh, G.; Del Pópolo, M. G.; Jones, J. T. A.; Hasell, T.; Cooper, A. I.; Horton, P. N.; Hursthouse, M. B.; James, S. L. *Chem. Sci.* **2012**, *3*, 2153.
(9) (a) Cram, D. J.; Karbach, S.; Kim, Y. H.; Baczynskyj, L.; Kalleymeyn, G. W. *J. Am. Chem. Soc.* **1985**, *107*, 2575. (b) Cram, D. J.; Karbach, S.; Kim, Y. H.; Baczynskyj, L.; Marti, K.; Sampson, R. M.; Kelleymeyn, G. W. *J. Am. Chem. Soc.* **1988**, *110*, 2554. (c) Sherman, J. C.; Cram, D. J. *J. Am. Chem. Soc.* **1989**, *111*, 4527. (d) Jasat, A.; Sherman, J. C. *Chem. Rev.* **1999**, 99. (e) Roach, P.; Warmuth, R. *Angew. Chem., Int. Ed.* **2003**, *42*, 3039. (f) Makeiff, D. A.; Sherman, J. C. *J. Am. Chem. Soc.* **2005**, *127*, 12363. (g) Ihm, C.; Jo, E.; Kim, J.; Paek, K. *Angew. Chem., Int. Ed.* **2006**, *45*, 20569. (h) Chen, J. Y.-C.; Jayaraj, N.; Jockusch, S.; Ottaviani, M. F.; Ramamurthy, V.; Turro, N. J. *J. Am. Chem. Soc.* **2008**, *130*, 7206. (i) Srinivasan, K.; Gibb, B. C. *Chem. Commun.* **2008**, *38*, 4640. (j) Wang, H.; Liu, F.; Helgeson, R. C.; Houk, K. N. *Angew. Chem., Int. Ed.* **2013**, *52*, 655.
(10) (a) Cram, D. J.; Tanner, M. E.; Knobler, C. B. *J. Am. Chem. Soc.* **1991**, *113*, 7717. (b) Cram, D. J.; Jaeger, R.; Deshayes, K. *J. Am. Chem. Soc.* **1993**, *115*, 10111. (c) Makeiff, D. A.; Pope, D. J.; Sherman, J. C. *J. Am. Chem. Soc.* **2000**, *122*, 1337. (d) Warmuth, R.; Yoon, J. *Acc. Chem. Res.* **2001**, *34*, 95. (e) Warmuth, R.; Makowiec, S. *J. Am. Chem. Soc.* **2007**, *129*, 1233. (f) Lu, Z.; Moss, R. A.; Warmuth, R.; Krogh-Jespersen, K. *J. Phys. Chem. A* **2011**, *115*, 13799. (g) Li, M.-J.; Huang, C.-H.; Lai, C.-C.; Chiu, S.-H. *Org. Lett.* **2012**, *14*, 6146. (h) Lin, Z.; Sun, J.; Efremovska, B.; Warmuth, R. *Chemistry* **2012**, *18*, 12864.
(11) (a) Cram, D. J.; Tanner, M. E.; Knobler, C. B. *J. Am. Chem. Soc.* **1991**, *113*, 7717. (b) Cram, D. J. *Nature* **1992**, *356*, 29. (c) Cram, D. J.; Cram, J. M. Container Molecules and their Guests. In *Monographs in Supramolecular Chemistry*; Stoddart, J. F., Ed.; Royal Society of Chemistry: Cambridge, 1994. Just as when cryptands form complexes, they are called cryptates, spherands, carcerands, and hemicarcerands are referred to as spheraplexes, carceplexes, and hemicarceplexes, respectively.
(12) Cram, D. J. *Angew. Chem., Int. Ed. Engl.* **1988**, *27*, 1009.
(13) Concurrently with the advent of cage-like host molecules, there was a dramatic growth in cage-like supermolecules where their outer shells are held together by noncovalent bonding interactions. Cram's so-called velcraplexes are early examples of supramolecular hosts where the driving forces for their formation are both solvophobic (enthalpic) and entropic. See: Cram, J. J.; Choi, H.-J.; Bryant, J. A.; Knobler, C. B. *J. Am. Chem. Soc.* **1992**, *114*, 7748. The field of cage-like supermolecules was one that was largely pioneered by Rebek who has employed multiple and cooperative hydrogen bonding interactions in order to create self-assembling capsules for the most part in organic solvents. See: (a) King, J. M.; Rebek, J. *Nature* **1996**, *382*, 239. (b) Conn, M. M.; Rebek, J. *Chem. Rev.* 1997, *97*, 1647. (c) Rebek, J. *Acc. Chem. Res.* **1999**, *32*, 278. (d) Hof, F.; Craig, S. L.; Nuckolls, C.; Rebek, J. *Angew. Chem., Int. Ed.* **2002**, *41*, 1488. (e) Ajami, D.; Rebek, J. *Top. Curr. Chem.* **2012**, *319*, 57.
(14) (a) Diederich, F.; Dick, K. *Angew. Chem., Int. Ed. Engl.* **1984**, *23*, 810. (b) Diederich, F.; Dick, K.; Griebel, D. *J. Am. Chem. Soc.* **1986**, *108*, 2273. (c) O'Krongly, D.; Denmeade, S. R.; Chiang, M. Y.; Breslow, R. *J. Am. Chem. Soc.* **1985**, *107*, 5544. (d) Seel, C.; Vögtle, F. *Angew. Chem., Int. Ed. Engl.* **1992**, *31*, 528. (e) Chapman, R. G.; Sherman, J. C. *J. Am. Chem. Soc.* **1998**, *120*, 9818. (f) Marchand, A. P. *Science* **2003**, *299*, 52. (g) Gibb, C. L. D.; Gibb, B. C. *J. Am. Chem. Soc.* **2004**, *126*, 11408. (h) Komatsu, K.; Murata, M.; Murata, Y. *Science* **2005**, *307*, 238. (i) Liu, X.; Liu, Y.; Li, G.; Warmuth, R. *Angew. Chem., Int. Ed.* **2006**, *45*, 901. (j) Liu, Y.; Liu, X.; Warmuth, R. *Chem. Eur. J.* **2007**, *13*, 8953. (k) Xu, D.; Warmuth, R. *J. Am. Chem. Soc.* **2008**, *130*, 7520. (l) Tozawa, T.; Jones, J. T. A.; Swamy, S. I.; Jiang, S.; Adams, D. J.; Shakespeare, S.; Clowes, R.; Bradshaw, D.; Hasell, T.; Chong, S.; Tang, C.; Thompson, S.; Parker, J.; Trewin, A.; Bacsa, J.; Slawin, A. M. Z.; Steiner, A.; Cooper, A. I. *Nat. Mater.* **2009**, *8*, 973. (m) Cooper, A. I. *Angew. Chem., Int. Ed.* **2011**, *50*, 996. (n) Popov, A. A.; Yang, S.; Dunsch, L. *Chem. Rev.* **2013**, *113*, 5989. (o) Hasell, T.; Culshaw, J. L.; Chong, S. Y.; Schmidtmann, M.; Little, M. A.; Jelfs, K. E.; Pyzer-Knapp, E. O.; Shepherd, H.; Adams, D. J.; Day, G. M.; Cooper, A. I. *J. Am. Chem. Soc.* **2014**, *136*, 1438.
(15) (a) Fujita, M.; Nagao, S.; Ogura, K. *J. Am. Chem. Soc.* **1995**, *117*, 1649. (b) Beissel, T.; Powers, R. E.; Raymond, K. N. *Angew. Chem., Int. Ed.* **1996**, *35*, 1084. (c) Stang, P. J.; Olenyuk, B.; Muddiman, D. C.; Smith, R. D. *Organometallics* **1997**, *16*, 3094. (d) Olenyuk, B.; Whiteford, J. A.; Fechtenkötter, A.; Stang, P. J. *Nature* **1999**, *398*, 796. (e) Fujita, M.; Umemoto, K.; Yoshizawa, M.; Fujita, N.; Kusukawa, T.; Biradha, K. *Chem. Commun.* **2001**, 509. (f) Dalgarno, S. J.; Power, N. P.; Atwood, J. L. *Coord. Chem. Rev.* **2008**, *252*, 825. (g) Mal, P.; Schultz, D.; Beyeh, K.; Rissanen, K.; Nitschke, J. R. *Angew. Chem., Int. Ed.* **2008**, *47*, 8297. (h) Pluth, M. D.; Bergman, R. G.; Raymond, K. N. *Acc. Chem. Res.* **2009**, *42*, 1650. (i) Chakrabarty, R.; Mukherjee, P. S.; Stang, P. J. *Chem. Rev.* **2011**, *111*, 6810. (j) Kumari, H.; Mossine, A. V.; Kline, S. R.; Dennis, C. L.; Fowler, D. A.; Teat, S. J.; Barnes, C. L.; Deakyne, C. A.; Atwood, J. L. *Angew. Chem., Int. Ed.* **2012**, *51*, 1452. (k) Fujita, D.; Suzuki, K.; Sato, S.; Yagi-Utsumi, M.; Yamaguchi, Y.; Mizuno, N.; Kumasaka, T.; Takata, M.; Noda, M.; Uchiyama, S.; Kato, K.; Fujita, M. *Nat. Commun.* **2012**, *3*, 1093. (l) Ma, S.; Smulders, M. M. T.; Hristova, Y. R.; Clegg, J. K.; Ronson, T. K.; Zarra, S.; Nitschke, J. R. *J. Am. Chem. Soc.* **2013**, *135*, 5678.
(16) (a) Vögtle, F.; Müller, W. M.; Werner, U.; Losensky, H. W. *Angew. Chem., Int. Ed. Engl.* **1987**, *26*, 901. (b) Dalgarno, S. J.; Tucker, S. A.; Bassil, D. B.; Atwood, J. L. *Science* **2005**, *309*, 2037. (c) Liu, S.; Gan, H.; Hermann, T.; Trick, S. W.; Gibb, B. C. *Nat. Chem.* **2010**, *2*, 847. (d) Mitra, T.; Jelfs, K. E.; Schmidtmann, M.; Ahmed, A.; Chong, S. Y.; Adams, D. J.; Cooper, A. I. *Nat. Chem.* **2013**, *19*, 8378.
(17) (a) Parsons, S.; Solan, G. A.; Winpenny, R. E. P.; Benelli, C. *Angew. Chem., Int. Ed. Engl.* **1996**, *35*, 1825. (b) Woodruff, D. N.; Winpenny, R. E. P.; Layfield, R. A. *Chem. Rev.* **2013**, *113*, 5110. (c) Blagg, R. J.; Ungur, L.; Tuna, F.; Speak, J.; Comar, P.; Collison, D.;

Wernsdorfer, W.; McInnes, E. J. L.; Chibofaru, L. F.; Winpenny, R. E. P. *Nat. Chem.* **2013**, *5*, 673.
(18) (a) Cook, T. R.; Vajpayee, V.; Lee, M. H.; Stang, P. J.; Chi, K.-W. *Acc. Chem. Res.* **2013**, *46*, 2464. (b) Therrien, B. *Chem. Eur. J.* **2013**, *19*, 8378.
(19) (a) Cram, D. J.; Tanner, M. E.; Thomas, R. *Angew. Chem., Int. Ed. Engl.* **1991**, *30*, 1024. (b) Warmuth, R. *Angew. Chem., Int. Ed. Engl.* **1997**, *36*, 1347. (c) Warmuth, R.; Marvel, M. A. *Angew. Chem., Int. Ed.* **2000**, *39*, 1117. (d) Liu, X.; Chu, G.; Moss, R. A.; Sauers, R. R.; Warmuth, R. *Angew. Chem., Int. Ed.* **2005**, *44*, 1994. (e) Natarajan, A.; Kaanumalle, L. S.; Jockusch, S.; Gibb, C. L. D.; Gibb, B. C.; Turro, N. J.; Ramamurthy, V. *J. Am. Chem. Soc.* **2007**, *129*, 4132. (f) Pluth, M. D.; Berman, R. G.; Raymond, K. N. *Science* **2007**, *316*, 85. (g) Yoshizawa, M.; Klosterman, J. K.; Fujita, M. *Angew. Chem., Int. Ed.* **2009**, *48*, 3418. (h) Mal, P.; Breiner, B.; Rissanen, K.; Nitschke, J. R. *Science* **2009**, *324*, 1697. (i) Hastings, C. J.; Bergman, R. G.; Raymond, K. N. *Chem. Eur. J.* **2014**, *20*, 3966.
(20) (a) Barnes, J. C.; Juríček, M.; Strutt, N. L.; Frasconi, M.; Sampath, S.; Giesener, M. A.; McGrier, P. L.; Bruns, C. J.; Stern, C. L.; Sarjeant, A. A.; Stoddart, J. F. *J. Am. Chem. Soc.* **2013**, *135*, 183. (b) Juríček, M.; Barnes, J. C.; Dale, E. J.; Liu, W.-G.; Strutt, N. L.; Bruns, C. J.; Vermeulen, N. A.; Ghooray, K. C.; Sarjeant, A. A.; Stern, C. L.; Botros, Y. Y.; Goddard, W. A., III; Stoddart, J. F. *J. Am. Chem. Soc.* **2013**, *135*, 12736. (c) Barnes, J. C.; Juríček, M.; Vermeulen, N. A.; Dale, E. J.; Stoddart, J. F. *J. Org. Chem.* **2013**, *78*, 11962.
(21) (a) Anderson, S.; Anderson, H. L.; Sanders, J. K. M. *Acc. Chem. Res.* **1993**, *26*, 469. (b) Cacciapaglia, R.; Mandolini, L. *Chem. Soc. Rev.* **1993**, *22*, 221. (c) Hoss, R.; Vögtle, F. *Angew. Chem., Int. Ed. Engl.* **1994**, *33*, 375. (d) Hubin, T. J.; Busch, D. H. *Coord. Chem. Rev.* **2000**, *200*, 5. (e) Meyer, C. D.; Joiner, C. S.; Stoddart, J. F. *Chem. Soc. Rev.* **2007**, *36*, 1705. (f) Crowley, J. D.; Goldup, S. M.; Lee, A. L.; Leigh, D. A.; McBurney, R. T. *Chem. Soc. Rev.* **2009**, *38*, 1530.
(22) (a) Odell, B.; Reddington, M. V.; Slawin, A. M. Z.; Spencer, N.; Stoddart, J. F.; Williams, D. J. *Angew. Chem., Int. Ed. Engl.* **1988**, *27*, 1547. (b) Ashton, P. R.; Odell, B.; Reddington, M. V.; Slawin, A. M. Z.; Stoddart, J. F.; Williams, D. J. *Angew. Chem., Int. Ed. Engl.* **1988**, *27*, 1550. (c) Asakawa, M.; Dehaen, W.; L'abbé, G.; Menzer, S.; Nouwen, J.; Raymo, F. M.; Stoddart, J. F.; Williams, D. J. *J. Org. Chem.* **1996**, *61*, 9591. (d) Sue, C.-H.; Basu, S.; Fahrenbach, A. C.; Shveyd, A. K.; Dey, S. K.; Botros, Y. Y.; Stoddart, J. F. *Chem. Sci.* **2010**, *1*, 119. (e) Barnes, J. C.; Fahrenbach, A. C.; Dyar, S. M.; Frasconi, M.; Giesener, M. A.; Zhu, Z.; Hartlieb, K. J.; Carmieli, R.; Wasielewski, M. R.; Stoddart, J. F. *Proc. Natl. Acad. Sci. U.S.A.* **2012**, *109*, 11446.
(23) Doomavanov, O. V.; Bourhis, L. J.; Gildea, J. A.; Howard, J. A. K.; Puschmann, H. *J. Appl. Crystallogr.* **2009**, *42*, 339.
(24) Sheldrick, G. M. *Acta Crystallogr.* **2008**, *A64*, 112.
(25) Thorn, A.; Dittrich, B.; Sheldrick, G. M. *Acta Crystallogr.* **2012**, *A68*, 448.
(26) Spek, A. *J. Appl. Crystallogr.* **2003**, *36*, 7.
(27) (a) McGarrity, J. F.; Prodolliet, J.; Smyth, T. *Org. Magn. Reson.* **1981**, *17*, 59. (b) Denmark, S. E.; Williams, B. J.; Eklov, B. M.; Pham, S. M.; Beutner, G. L. *J. Org. Chem.* **2010**, *75*, 5558.
(28) For an early example of this conceptual comparison, see: Curtis, W. D.; Stoddart, J. F.; Jones, G. H. *J. Chem. Soc., Perkin Trans. I* **1977**, *7*, 785.
(29) Schmittel, M.; He, B.; Mal, P. *Org. Lett.* **2008**, *10*, 2513.
(30) (a) Miljanić, O. Š.; Stoddart, J. F. *Proc. Natl. Acad. Sci. U.S.A.* **2007**, *104*, 12966. (b) Patel, K.; Miljanić, O. Š.; Stoddart, J. F. *Chem. Commun.* **2008**, *16*, 1853.
(31) Marinov, N. M.; Pitz, W. J.; Westbrook, C. K.; Castaldi, M. J.; Senkan, S. M. *Combust. Sci. Technol.* **1996**, *116*, 211.
(32) (a) Faraday, M. *Philos. Trans. R. Soc. London* **1825**, *115*, 440. (b) Radziszewski, B. *Ber. Dtsch. Chem.* **1876**, *9*, 260.
(33) (a) Tang, J.; Carroquino, M. J.; Robertson, B. K.; Alexander, M. *Environ. Sci. Technol.* **1998**, *32*, 3586. (b) Ghosh, U.; Gillette, J. S.; Luthy, R. G.; Zare, R. N. *Environ. Sci. Technol.* **2000**, *34*, 1729. (c) Boström, C.-E.; Gerde, P.; Hanberg, A.; Jernström, B.; Johansson, C.; Kyoklund, T.; Rannug, A.; Tornqvist, M.; Vietorin, K.; Westerholm, R. *Environ. Heal. Perspect.* **2002**, *110*, 451. (d) Werner, D.; Higgins, C. P.; Luthy, R. G. *Water Res.* **2005**, *32*, 2105.
(34) Li, X.; Liu, X.; Zhang, L.; You, L.; Zhao, J.; Wu, H. *Environ. Toxicol. Pharmacol.* **2011**, *32*, 373.
(35) Current Occupational Safety and Health Administration (OSHA) Standards are set at 10 ppm averaged over an 8 h work period.
(36) (a) Abdo, K. M.; Eustis, S. L.; McDonald, M.; Jokinen, M. P.; Adkins, B.; Haseman, J. K. *Inhal. Toxicol.* **1992**, *4*, 393. (b) Preuss, R.; Augerer, J.; Drexler, H. *Int. Arch. Occup. Environ. Health* **2003**, *76*, 556. (c) North, D. W.; Abdo, K. M.; Benson, J. M.; Dahl, A. R.; Morris, J. B.; Renne, R.; Witschi, H. *Regul. Toxicol. Pharmacol.* **2008**, *51*, 56.
(37) Naphthalene is the major single component in coal tar at ca. 10%; 1.3 million tons are produced annually. It is used in the production of, for example, phthalic anhydride, moth balls, and the insecticide, carbaryl.
(38) (a) Blyshak, L. A.; Dodson, K. Y.; Patonay, G.; Warner, I. M. *Anal. Chem.* **1989**, *61*, 955. (b) Mohseni, R. M.; Hurtubise, R. J. *J. Chromatogr., A* **1990**, *499*, 395. (c) Lamparczyk, H.; Zarzycki, P.; Ochocka, R. J.; Sybilska, D. *Chromatographia* **1990**, *30*, 91. (d) Butterfield, M. T.; Agbaria, R. A.; Warner, I. M. *Anal. Chem.* **1996**, *68*, 1187. (e) Shixiang, G.; Liansheng, W.; Qiugguo, H.; Sukui, H. *Chemosphere* **1998**, *37*, 1299. (f) Ravelet, C.; Ravel, A.; Grosset, C.; Villet, A.; Geze, A.; Wouessidjewe, D.; Peyrin, E. *J. Liq. Chromatogr. Relat. Technol.* **2002**, *25*, 421. (g) Choi, Y.; Cho, Y.-M.; Gala, W. R.; Luthy, R. G. *Environ. Sci. Technol.* **2013**, *47*, 1024.
(39) (a) Yoshizawa, M.; Nakagawa, J.; Kumazawa, K.; Nagao, M.; Kawano, M.; Ozeki, T.; Fujita, M. *Angew. Chem., Int. Ed.* **2005**, *44*, 1810. (b) Peinador, C.; Pía, E.; Blanco, V.; Garcia, M. D.; Quintela, J. M. *Org. Lett.* **2010**, *12*, 1380. (c) Blanco, V.; García, M. D.; Terenzi, A.; Pía, E.; Fernández-Mato, A.; Peinador, C.; Quintela, J. M. *Chem. Eur. J.* **2010**, *16*, 12373. (d) Therrin, B. *Chem. Eur. J.* **2013**, *19*, 8378.
(40) In a landmark paper published in 1998, Rebek has presented evidence that "molecular recognition through encapsulation processes is largely determined by the volumes of the guest and host. Binding of molecules of suitable dimensions in the internal cavity of a molecular receptor in solution can be expected when the packing coefficient, the ratio of guest volume to host volume is in the range of 0.55 ± 0.09. Larger packing coefficients up to 0.70 can be reached if the complex is stabilized by strong intermolecular forces such as hydrogen bonds". He goes on to add that "Guest design based on volume and shape considerations only gives good results with the weakest forces: dipole−dipole, dipole−induced dipole, and London dispersion forces." In the context of **ExCage**$^{6+}$, which is replete with potential molecular recognition in the shape of both face-to-face and edge-to-face $\pi-\pi$ stacking interactions when forming 1:1 complexes, it is clear that the packing coefficients are going to exceed 0.55, particularly in the case of the larger PAHs. This sentiment is aligned with Rebek's expectation that, "Encapsulation of bigger guests can, however, be attained by extra stabilization from additional intermolecular interactions such as hydrogen bonds". See: Mecozzi, S.; Rebek, J., Jr. *Chem. Eur. J.* **1998**, *4*, 1016.
(41) ImageJ v1.48 was used to trace the outline of each shape and obtain the surface area overlap (SAO) between the host and each guest (Figure S30). The SAO-**ExCage**$^{6+}$ was determined by dividing the SAO by the total available binding area of **ExCage**$^{6+}$, while the SAO-PAH was determined by dividing the SAO by the total area of the PAH. On account of the relative planarity of both the host and guest upon complexation, this model can be used to estimate the percent volume occupancy by extending this overlap into the third dimension. Using this model, the guest-accessible volume of the binding cavity of **ExCage**$^{6+}$ was obtained. The occupied portions in each complex were calculated by multiplying the volume of the guest (using the average value of the MarvinSketch and VEGA ZZ programs) by the SAO-PAH, while the unoccupied contribution was calculated by dividing the resulting value by the SAO-**ExCage**$^{6+}$. See Section F in the Supporting Information for additional experimental details.
(42) *Health Effects Support Document for Naphthalene*, EPA 822-R-03-005; Office of Water, U. S. EPA: Washington, DC, 2003; retrieved from http://water.epa.gov/action/advisories/drinking/upload/2003_03_05_support_cc1_naphthalene_healtheffects.pdf (accessed June 2, 2014).

(43) It should be noted that a distortion is evident in the solid-state structure of coronene⊂**ExCage**$^{6+}$. While most inclusion complexes examined appeared to pack similarly in the solid-state superstructure, coronene⊂**ExCage**$^{6+}$ deviates from this trend, presumably because of the size-induced conformational change. For the solid-state structures, see Supporting Information.

(44) (a) Nakamura, K.; Houk, K. N. *J. Am. Chem. Soc.* **1995**, *117*, 1853. (b) Houk, K. N.; Nakamura, K.; Sheu, C.; Keating, A. E. *Science.* **1996**, *273*, 627. (c) Helgeson, R. C.; Hayden, A. E.; Houk, K. N. *J. Org. Chem.* **2010**, *75*, 570. (d) See Ref 9.j;. (e) Liu, F.; Helgeson, R. C.; Houk, K. N. *Acc. Chem. Res.* **2014**, in press.

(45) (a) Jiang, Y.; Lee, A.; Chen, J.; Cadene, M.; Chait, B. T.; MacKinnon, R. *Nature* **2002**, *417*, 523. (b) Perozo, E.; Cortes, D. M.; Sompornpisut, P.; Kloda, A.; Martinac, B. *Nature* **2002**, *418*, 942.

(46) Although the ΔG^0 values at −5.59, −6.88, −7.95, and −8.52 kcal mol^{-1} for the binding by **ExCage**$^{6+}$ of phenanthrene, pyrene, triphenylene, and perylene, respectively, in DMF are not significantly different (Table 3) from those (ΔG^0 = −5.34, −7.95, −8.27, and −9.20 kcal mol^{-1}, respectively) in MeCN (Table 1), both the enthalpies and entropies of binding differ considerably, yet in such a manner that the effects cancel each other out. We suspect that solvophobic forces are more dominant in DMF than MeCN.

(47) On account of the fact that phenanthrene can only access two binding pockets at any one time, the enhancement provided by the macrobicyclic effect is impaired.

(48) (a) Cram, D. J.; Blanda, M. T.; Paek, K.; Knobler, C. B. *J. Am. Chem. Soc.* **1992**, *114*, 7765. (b) See ref 41.